UNIVERSITAT POLITÈCNICA DE VALÈNCIA

Escola Tècnica Superior d'Enginyeria Agronòmica i del Medi Natural

UNIVERSITAT POLITÈCNICA DE VALÈNCIA

School of Agricultural Engineering and Environment

Molecular function of Insulin Receptor Substrate 2 (Irs2) in mouse trophoblast stem cells

End of Degree Project

Bachelor's Degree in Biotechnology

AUTHOR: Moya Navamuel, Maria

Tutor: Giraldo Reboloso, Esther

Experimental director: PEREZ GARCIA, VICENTE

ACADEMIC YEAR: 2022/2023

MOLECULAR FUNCTION OF INSULIN RECEPTOR SUBSTRATE 2 (*Irs2*) IN MOUSE TROPHOBLAST STEM CELLS

Bachelor's thesis
Bachelor's Degree in Biotechnology
Academic year 2022/2023
Universitat Politècnica de València
Escuela Técnica Superior de Ingeniería Agronómica y del Medio Natural

Author: María Moya Navamuel

Academic tutor: Dr. Esther Giraldo Reboloso

Experimental director: Dr. Vicente Pérez García

Valencia, June 2023

Title

Molecular function of Insulin Receptor Substrate 2 (*Irs2*) in mouse trophoblast stem cells

Título

Función molecular del Sustrato del Receptor de Insulina 2 (*Irs2*) en células madre trofoblásticas de ratón

Títol

Funció molecular del Substrat del Receptor de la Insulina 2 (*Irs2*) en cèl·lules mare trofoblàstiques de ratolí

Abstract

The placenta is a transient yet vital organ that allows the exchange of oxygen and nutrients between the mother and the fetus during gestation. Formation of the placenta is a complex and highly regulated process that is essential for mammalian development. It relies on the differentiation of extraembryonic cells into specialized trophoblast lineages that constitute the building blocks of the placenta. Defects in placental development are associated with maternal pregnancy disorders such as gestational diabetes mellitus (GDM) and pre-eclampsia, as well as fetal complications including fetal insulin resistance and fetal growth restriction (FGR). Despite extensive research on placental development, the molecular mechanisms governing placental formation and trophoblast cell lineage differentiation are poorly understood.

Insulin receptor substrate 2 (IRS2) is a signaling protein that plays a crucial role in insulin and insulin-like growth factor (IGF) signaling pathways. This cytoplasmic adaptor protein binds to activated tyrosine kinase receptors, including the insulin receptor (IR) and insulin-like growth factor 1 receptor (IGF1R). Without associated catalytic activity, IRS2 can trigger the activation of the phosphatidylinositol 3-kinase (PI3K/AKT) and mitogen-activated Ras-protein kinase (MAPK) signaling pathways. Despite prior research on the biological functions of IRS2, its involvement in placental development remains unexplored.

In this work, we shed light on the molecular function of *Irs2* in mouse trophoblast stem cells (mTSCs). To achieve this objective, we firstly analyzed the dynamics of IRS2 expression by conducting a 6-day time course differentiation experiment. Our findings indicate that IRS2 expression is modulated during trophoblast differentiation, suggesting that it contributes to placental development.

To further investigate the role of IRS2 in regulating placentation, we characterized *Irs2* CRISPR/Cas9 KO mTSCs generated previously in the laboratory. For this purpose, we performed RNAseq analysis and compared the transcriptome at 0, 3 and 6 days of trophoblast differentiation of *Irs2*-null mTSCs to control cells. Our results show that IRS2 depletion affects late trophoblast differentiation events.

With the aim of delineating and dissecting the IRS2-mediated signaling pathways related to these defects, we performed signaling experiments by stimulating starved mTSCs with IGFs, factors implicated in placental growth. Our data indicate that *Irs2* KO mTSCs exhibit delayed activation of the PI3K/AKT pathway upon IGF2 stimulation, similarly to the results obtained when stimulating with IGF1. This suggests that IGF2 and IGF1 have overlapping roles, signaling through IGF1R to control trophoblast proliferation and differentiation. These findings provide new insights into the pathways signaling through IRS2 in mTSCs and represent a significant advance in our understanding of placental development.

The following work is related mainly to the Sustainable Development Goal (SDG) 3 within the 2030 Agenda: Good Health and Well-being, but also in some extent to the SDG 4, 5 and 10 (Appendix I). It contributes to understanding the molecular mechanisms underlying pregnancy complications, thereby, potentially improving maternal and child health outcomes.

Resumen

La placenta es un órgano vital y transitorio que permite el intercambio de oxígeno y nutrientes entre madre y feto durante la gestación. La placentación es un proceso complejo, altamente regulado, esencial para el desarrollo del mamífero. Depende de la diferenciación de células extraembrionarias hacia linajes trofoblásticos especializados, los principales pilares de la placenta. Defectos en su desarrollo se asocian con complicaciones del embarazo, como diabetes mellitus gestacional (DMG) y preeclampsia; así como con complicaciones fetales, como resistencia a la insulina y restricción del crecimiento fetal (RCF). A pesar de la extensa investigación sobre el desarrollo placentario, los mecanismos moleculares que rigen la placentación son poco comprendidos.

El sustrato del receptor de insulina 2 (IRS2) es una proteína de señalización que desempeña un papel crucial en las vías de señalización de la insulina y factores de crecimiento similares a la insulina (IGFs). Este adaptador citoplásmico se une a receptores tirosina quinasa activos, incluyendo el receptor de insulina (IR) y el receptor de IGF1 (IGF1R). Sin actividad catalítica asociada, IRS2 es capaz de activar la señalización de la fosfatidilinositol 3-quinasa (PI3K/AKT) y la quinasa de proteína Ras activada por mitógenos (MAPK). A pesar de investigación previa sobre las funciones biológicas de IRS2, su participación en el desarrollo placentario sigue sin explorarse.

En este trabajo, dilucidamos la función molecular de *Irs2* en células madre trofoblásticas de ratón (mTSCs). Para lograr este objetivo, primero analizamos la dinámica de expresión de IRS2 mediante un experimento de 6 días de diferenciación. Nuestros hallazgos indican que la expresión de IRS2 se modula durante la diferenciación del trofoblasto, lo que sugiere que contribuye al desarrollo placentario.

Para investigar aún más el papel de IRS2 en la regulación de la placentación, caracterizamos las mTSCs KO para *Irs2* generadas previamente en el laboratorio con CRISPR/Cas9. Para este propósito, realizamos un análisis de RNAseq y comparamos el transcriptoma en 0, 3 y 6 días de diferenciación de células KO y control. Nuestros resultados muestran que la ausencia de IRS2 afecta la diferenciación trofoblástica tardía.

Con el objetivo de delinear y desglosar las vías de señalización mediadas por IRS2 relacionadas con estos defectos, estimulamos mTSCs con IGFs, factores implicados en el crecimiento placentario. Nuestros datos indican que las mTSCs KO para *Irs2* muestran una activación retrasada de la vía PI3K/AKT tras la estimulación con IGF2, resultados similares a los obtenidos tras estimular con IGF1. Esto sugiere que IGF2 e IGF1 tienen roles redundantes, señalando a través de IGF1R para controlar la proliferación y diferenciación trofoblástica. Estos hallazgos proporcionan nuevas ideas sobre las vías de señalización a través de IRS2 en las células madre trofoblásticas de ratón y representan un avance significativo en nuestra comprensión del desarrollo placentario.

Este trabajo se relaciona mayoritariamente con el Objetivo de Desarrollo Sostenible (ODS) 3 de la Agenda 2030: Salud y Bienestar, aunque también con el 4, 5 y 10 (Anexo I). Contribuye a comprender los mecanismos moleculares que subyacen a las complicaciones durante el embarazo, lo que podría mejorar la salud materna e infantil.

Key words

Placenta, mouse trophoblast stem cells, *Irs2*, insulin/IGF axis, signaling pathways

Palabras clave

Placenta, células madre trofoblásticas de ratón, *Irs2*, eje insulina/IGF, vías de señalización

Author: María Moya Navamuel

Valencia, June 2023

Academic tutor: Dr. Esther Giraldo Reboloso

External cotutor: Dr. Vicente Pérez García

Acknowledgments/agradecimientos

Este proyecto marca un antes y un después en mi vida. Todo el esfuerzo y tiempo empleado, reflejado en estas páginas. Esfuerzo propio, tras cuatro años estudiando esta carrera tan bonita de biotecnología, además de esfuerzo de todas las personas que me han acompañado en esta etapa.

Primeramente, quería agradecerle a Vicen por confiar en mi y darme esta enorme oportunidad de aprender a su lado, que he exprimido al máximo. Gracias por apostar por mi y dejarme formar parte del equipo. Gracias por ser tan cercano, por tu atención y tu apoyo a lo largo del desarrollo del proyecto, que sé que no suele ser común en un IP.

Por supuesto, gracias a Mara, que ha hecho de este lugar un hogar. Mara, gracias por ayudarme mano a mano con todo, por enseñarme lo que es disfrutar del trabajo, con tu corazón tan grande y tu humor siempre tan auténtico. Gracias por quererme tanto y por ser tan paciente cuando me equivocaba. Además, gracias al resto del equipo del I-74: Paula, Ana, Marta, Eva y Sergio. Habéis hecho los días de trabajo más amenos, siempre que he bajado a la cafetería me lo he pasado genial con vosotros.

Por otra parte, quiero agradecer a mis amigos. Gracias Cris, Adri, Juanto, Carmen, Miguel y Capi, habéis hecho que mi etapa universitaria en la UPV haya sido divertida y llevadera. Extrañaré las tardes de cerves en bbaa, las meriendas en la Tarongería, las conversaciones tumbados en el césped de la ETSIAMN y las escapaditas a Jávea.

Asimismo, quiero darles las gracias a mis padres. Papá, Mamá, gracias por criarme como lo habéis hecho, siempre dispuestos a darlo todo por mi educación. Mamá, gracias por tu amor incondicional y cariño. Sé que estás muy orgullosa de mis logros, aunque en el fondo te entristece un poco que ya estoy saliendo de tu nido. No te preocupes, yo siempre seré tu niña bonita a la que cogías en brazos y le cantabas la Oreja de Van Gogh. Papá, gracias por tus consejos tan sabios y por enseñarme los valores que me han permitido alcanzar todas mis metas: “trabajo, constancia y dedicación”. Admiro mucho cómo eres, siempre has sido mi modelo a seguir y lo seguirás siendo. Por último, Gladys, gracias por siempre alegrarte por mis logros y tratarme como una hija más. Además, no pueden faltar mis queridos hermanos, Jimmy e Irene. No sería como soy hoy si no fuese por vosotros. Os quiero muchísimo a todos.

Por último, Eduardo, el amor de mi vida, mi compañerito de por siempre. Mi amor, gracias por sacar lo mejor de mi y por apoyarme emocionalmente. Gracias por tus palabras llenas de fuerza y energía para seguir luchando y no rendirme cuando todo parece ir mal. Como tú dices, al final nada es para tanto porque siempre acabo resolviéndolo. Gracias por haber sido testigo de mi esfuerzo y por haberme apoyado en todo momento, valorando todo lo que estoy haciendo. Gracias por darme tantas caricias, cocinarme tan tan tan rico y encargarte de las tareas domésticas durante estos meses de trabajo duro, que por suerte ya han terminado. Gracias por ser tan paciente y comprensivo. Eres un hombre lleno de amor y de bondad, súper inteligente y sensato, a lo que tengo a Rosa y Edison para agradecer. Te amo y siempre lo haré. Gracias de verdad.

Table of contents

List of acronyms and abbreviations

BSA: bovine serum albumin

Cas9: CRISPR-associated protein 9

CRISPR: clustered regularly interspaced short palindromic repeats

D: day of trophoblast differentiation

DAVID: Database for Annotation, Visualization and Integrated Discovery

DEGs: differentially expressed genes

E: day of embryonic development

EPC: ectoplacental cone

EPI: epiblast

ERK: extracellular signal-regulated kinase

ExE: extraembryonic ectoderm

ExM: extraembryonic mesoderm

FACS: fluorescence activated cell sorting

FBS: fetal bovine serum

FGF: fibroblast growth factor

FGR: fetal growth restriction

GDM: gestational diabetes mellitus GDM

GO: gene ontology

Grb2: growth factor receptor-bound protein 2

gRNA: guide RNA

HRP: horse radish peroxidase

ICM: inner cell-mass

IF: immunofluorescence

IGF: insulin-like growth factor

IGFBPs: insulin-like growth factor binding proteins

IGF1: insulin-like growth factor 1

IGF2: insulin-like growth factor 2

IGF1R: insulin-like growth factor 1 receptor

IR: insulin receptor

IR_A: insulin receptor isoform A

IRS2: insulin receptor substrate 2

IUGR: intrauterine growth restriction

KO: knockout

MAPK: mitogen-activated Ras-protein kinase

MEFs: mouse embryonic fibroblasts

mTE: mural trophectoderm

mTOR2: mammalian target of rapamycin complex 2

mTSCs: mouse trophoblast stem cells

NT: non-targeting

PBS: phosphate-buffered saline

PCA: principal component analysis

PDK1: phosphoinositide-dependent kinase 1

PE: primitive endoderm

PGH: placental growth hormone

PH: pleckstrin homology

PI3K: phosphatidylinositol 3-kinase

PIP_3: phosphatidylinositol-3, 4, 5-phosphate

PKB: protein kinase B (AKT)

PTB: phosphotyrosine binding

pTE: polar trophectoderm

PVDF: polyvinylidene difluoride

RT: room temperature

SDG: Sustainable Development Goal

SDS-PAGE: Sodium dodecyl-sulfate polyacrylamide gel electrophoresis

SEM: standard error of mean

SOS: son-of-sevenless

TE: trophectoderm

TF: transcription factor

TGCs: trophoblast giant cells

TGFß: transforming growth factor ß

TSCs: trophoblast stem cells

WB: Western Blot

WT: wild type

List of tables

List of figures

1. INTRODUCTION

1.1. Basic principles regarding the placenta

The placenta is a transient yet vital organ that provides an interface between the embryo and mother during gestation. As such, it allows to exchange oxygen, nutrients, metabolites and other molecules between them, sustaining the correct intrauterine fetus development. In addition to providing physical attachment to the uterine wall, it stimulates the production of pregnancy-sustaining hormones and creates an immune-privileged environment (Woods *et al.*, 2018). Due to its pivotal role in mammalian development, abnormalities in placentation are associated with pregnancy disorders such as gestational diabetes mellitus (GDM) and pre-eclampsia, as well as fetal complications including fetal insulin resistance and intrauterine growth restriction (IUGR) (Maltepe and Fisher, 2015).

Extensive research has been conducted on placental development and trophoblast cells, the building blocks of the placenta. Both mice and humans share a hemochorial placentation, in which the trophoblast invades extensively into the uterine wall, being in direct contact with maternal blood (Hemberger *et al*., 2020). Even if they have notable morphological differences and distinct placental cell lineages, they both present similar feto-maternal exchange regions: the chorionic villi for humans and the labyrinth for mice (Knöfler *et al*., 2019). Moreover, murine placentas exhibit three distinct and well-defined layers, rendering them highly manageable for manipulation. Lastly, they are easily genetically modified with well-established techniques (Renaud *et al*., 2011). Considering all of these benefits, the mouse is the most widely used animal model to study human pregnancy and the molecular mechanisms governing placentation.

1.1.1. Murine placental development

Formation of the placenta is a complex and highly regulated process that is essential for mammalian development. It relies on the differentiation of extraembryonic cells into specialized trophoblast lineages that constitute the essential elements of the placenta. However, it also involves contributions from certain cells with embryonic origin, the extraembryonic mesoderm (ExM), essential for the fetal placental vasculature formation. Both of these cell lineages derive from the fertilized oocyte and are established in the early development (Woods *et al*., 2018).

Once the mouse oocyte has been fertilized, the generated zygote undergoes a series of cell divisions, reaching the morula state at day 2.5 of embryonic development (E2.5). These eight cells will then continue to divide until blastocyst formation is accomplished at E3.5 (**Figure 1A**). At this developmental stage, cell polarity is classified into the intracellular mass (ICM) and the outer trophectoderm (TE). The ICM is composed of the primitive endoderm (PE) lineage, which will develop into the ExM, and the epiblast (EPI), which will give rise to the embryo proper (Hemberger *et al*., 2020). The TE cells can be divided into polar TE (pTE), which are in direct contact with the ICM, and mural TE (mTE), which surround the blastocoel (Maltepe and Fisher, 2015; Latos and Hemberger, 2016).

Further on in developmental time, the mTE will differentiate into primary trophoblast giant cells (TGCs), which exhibit invasive properties that allow them to initially attach the conceptus to the uterus. Implantation at E4.5 triggers the maternal decidualization, an adaptive process by which endometrial stromal fibroblasts become specialized secretory decidual cells during pregnancy to support fetal development (Hemberger *et al*., 2020). By E6.5, the pTE will give rise to the extraembryonic ectoderm (ExE) and the ectoplacental cone (EPC), closest to the implantation site (**Figure 1B**).

At this time point is when gastrulation takes place, forming three novel structures by E7.5: the EPI-derived amnion (sac to protect the embryo), the ExE-derived chorion and the ExM-derived allantois (**Figure 1C**). The allantois invaginates into the chorion, finally fusing together at around E8.5 (Woods *et al*., 2018). This enables the invagination of ExM-derived blood vessels into the chorionic trophoblast layer at E9.5, which is the first step to form the placental labyrinth.

Chorio-allantoic fusion (**Figure 2A**) is an obligate step, since it originates the exchange barrier by ensuring juxtaposition of fetal and maternal blood circulations (Maltepe and Fisher, 2015). These invasive mesodermal protrusions induce a differentiation process in the chorionic trophoblast, leading to the fusion of individual trophoblast cells to form syncytiotrophoblast (SynT) cells (Woods *et al*., 2018). This culminates in the mature labyrinth formation, composed of two separate SynT layers (SynT-I and SynT-II), juxtaposed sinusoidal trophoblast giant cells (TGCs) and endothelial cell of the fetal vasculature (Hemberger *et al*., 2020).

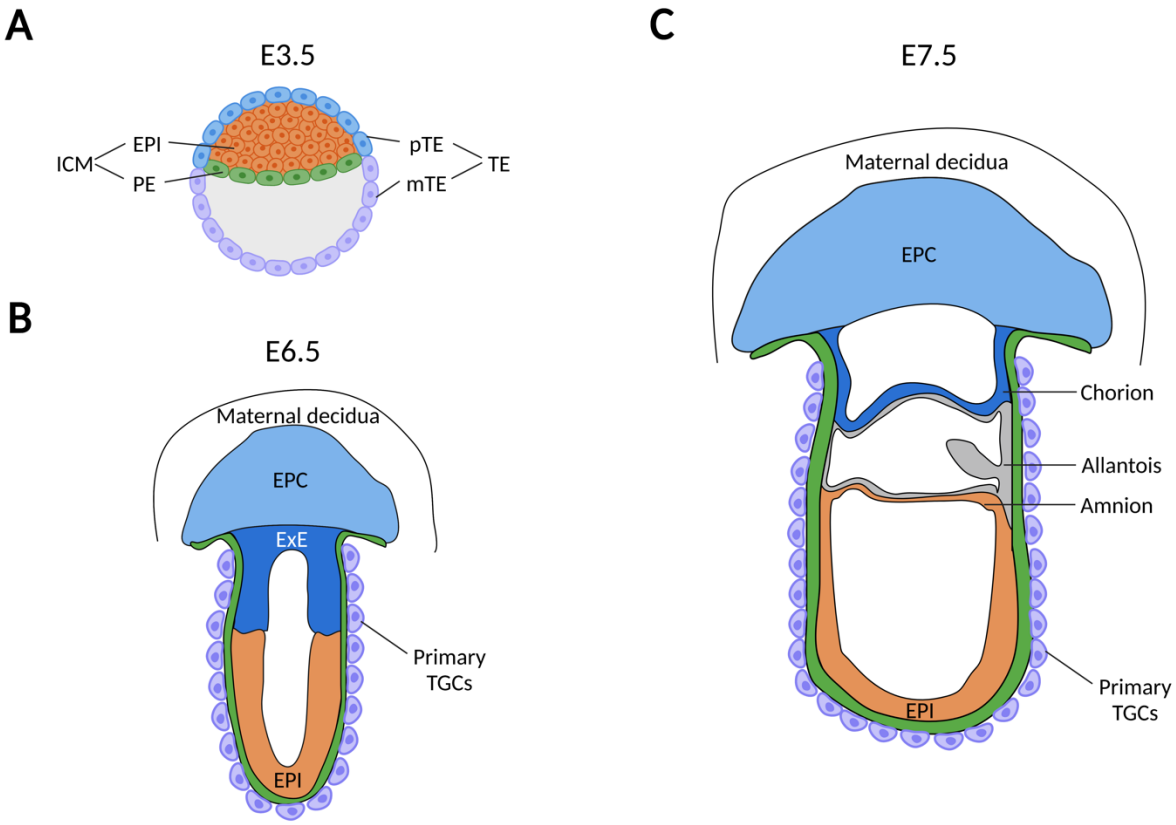

FIGURE 1. Early murine placental development. **(A)** Blastocyst structure accomplished at day 3.5 of embryonic development (E3.5). It is composed of the inner cell mass (ICM) and the trophectoderm (TE). The ICM can be divided into the epiblast (EPI) and the primitive endoderm (PE), while the TE can be divided into the polar TE (pTE) and the mural TE (mTE). **(B)** Succeeding implantation at E4.5, the blastocyst's mTE differentiates into primary trophoblast giant cells (TGCs), while the pTE gives rise to the extraembryonic ectoderm (ExE) and the ectoplacental cone (EPC) by E6.5. This structure is embedded into the maternal decidua which differentiates from the uterine endometrium. **(C)** Following gastrulation, the chorion, the allantois and the amnion form at E7.5. *Modified from Latos and Hemberger, 2016; Hemberger et al., 2020. Generated using Biorender.*

Furthermore, cells at the core of the EPC will differentiate into spongiotrophoblast (SpT) and glycogen trophoblast (GlyT) cells, important components of the junctional zone of the placenta (Woods *et al.*, 2016). Cells at the EPC's outer margins will differentiate into secondary TGCs, which include canal, parietal and spiral artery-associated TGCs (Latos and Hemberger, 2016). Finally, by E14.5, the chorioallantoic placenta is mature, grossly consisting of three layers: the labyrinth, the junctional zone (SpT, GlyT and parietal TGCs), and the maternal decidua (Hemberger *et al.*, 2020) (**Figure 2B**).

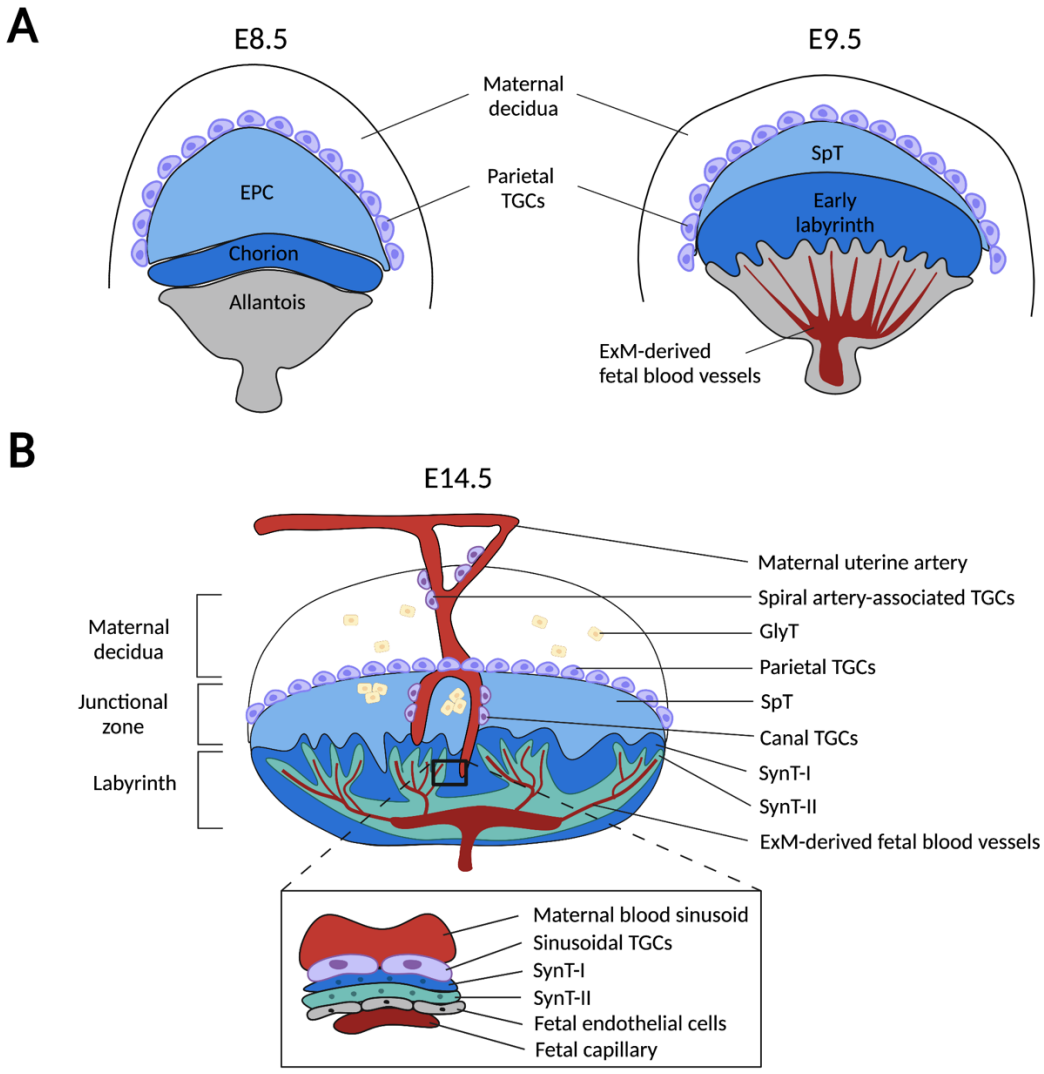

FIGURE 2. Late murine placental development. (A) At E8.5, the chorio-allantoic fusion takes place, resulting in the invagination of extraembryonic mesoderm (ExM)-derived fetal blood vessels into the chorion at E9.5. Moreover, cells in the ectoplacental cone (EPC) borders differentiate into secondary trophoblast giant cells (TGCs), including the parietal TGCs, (B) the spiral artery-associated TGCs, and the canal TGCs. Then the inner cells of the EPC derive into spongiotrophoblast (SpT) and glycogen trophoblast cells (GlyT). These differentiation processes establish the mature placenta at E14.5 showing the three main layers: the maternal decidua, the junctional zone (SpT, GlyT and parietal TGCs) and the labyrinth (exchange barrier between mother and fetus). *Modified from Latos and Hemberger, 2016. Generated using Biorender*

1.1.2. Trophoblast stem cells (TSCs)

Trophoblast stem cells (TSCs) are the precursors of the differentiated specialized trophoblast cell types of the placenta. They are a self-renewing stem cell population characterized by an indefinite proliferation potential and multipotency (Latos and Hemberger, 2014). This unique stem cell type can be derived in mice from the early trophoblast lineage, namely from pTE of the blastocyst or from ExE of early post-implantation conceptuses (Latos and Hemberger, 2016).

In vitro culture of mouse trophoblast stem cells (mTSCs) provides a valuable tool for investigating the molecular mechanisms underlying early placental development (Pérez-García *et al*., 2018). Insight can be gained by generating knockout (KO) TSC lines and studying their lineage commitment decisions. Moreover, mTSCs can serve as a model for placental-related disorders to observe implications of pregnancy complications (Maltepe and Fisher, 2015).

The maintenance of their multipotency and undifferentiated state *in vitro* is accomplished by culturing mTSCs in the presence of conditioned medium by mouse embryonic fibroblasts (MEFs), mitotically inactivated irradiated feeder cells which provide TGFß and Activin. This medium is supplemented with fibroblast growth factor (FGF) and heparin in order to sustain their self-renewal and proliferation potential (Roberts and Fisher, 2011; Latos and Hemberger, 2014). In the absence of these growth factors, mTSCs differentiate towards the different trophoblast cells types of the placenta, which can be identified by their corresponding molecular marker genes using WB or RT-qPCR analysis (**Figure 3**).

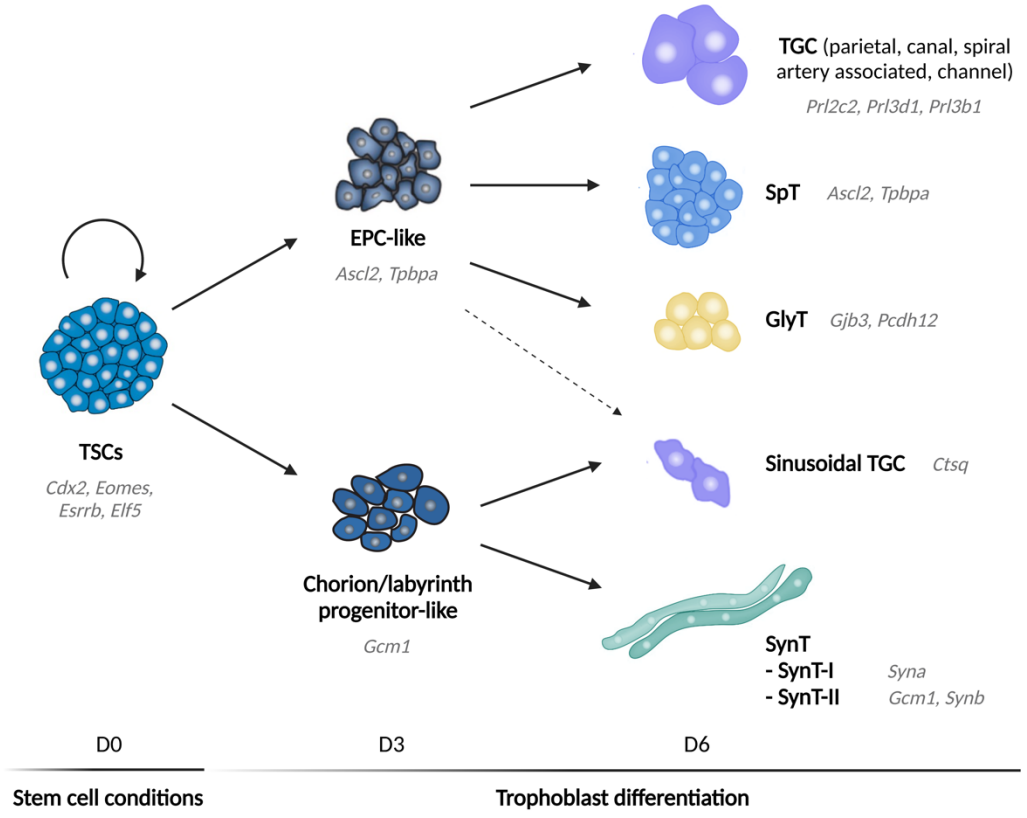

FIGURE 3. Trophoblast stem cell differentiation time course. Schematic representation of the different trophoblast cell types derived from trophoblast stem cells (TSCs) at day 3 (D3) and 6 (D6) of trophoblast differentiation, and their corresponding molecular marker genes. EPC, ectoplacental cone; GlyT, glycogen trophoblast cells; SpT, spongiotrophoblast; SynT, syncytiotrophoblast; TGC, trophoblast giant cells. *Modified from Pérez-García et al., 2018. Generated using Biorender.*

1.2. Insulin receptor substrate 2 (IRS2)

Insulin receptor substrate 2 (IRS2) is a cytoplasmic docking protein belonging to the insulin/insulin-like growth factor (IGF) signaling pathway. Even though it lacks intrinsic catalytic activity, it acts as an interface between activated insulin or IGF1 receptors (IR and IGF1R, respectively) and effector proteins downstream (Brummer *et al*., 2010). It mediates the activation of the phosphatidylinositol 3-kinase (PI3K)-AKT and the Ras-mitogen-activated protein kinase (MAPK) cascades through the insulin/IGF axis. Thus, this intracellular soluble protein regulates crucial biological processes, including glucose metabolism, protein synthesis and cell survival (Taniguchi *et al*., 2006).

1.2.1. Signaling through IRS2: the insulin/IGF axis

1.2.1.1. IRS2 as a cytosolic docking protein

IRS2 is a 1321-aminoacid long protein (185 kDa) encoded by the *Irs2* gene in the chromosome 8, containing 2 exons (NCBI, 2023). IRS2 belongs to a family of six members (IRS1-6), whose structure is made up of a highly-conserved N-terminal region containing a pleckstrin homology (PH) domain and a phosphotyrosine binding (PTB) domain, followed by a poorly-conserved C-terminal region with multiple tyrosine phosphorylation sites (UNIPROT, 2023). Phosphorylation of serine residues can also occur, serving as an inhibitory feedback mechanism (Sun *et al*., 1995). Another inhibitory mechanism is the action of the Scr homology 2 (SH2)-containing protein tyrosine phosphatase 2 (SHP2), which interacts with IRS2 via two phosphotyrosine residues at its C terminus and dephosphorylates the other phosphotyrosines that mediate the binding of PI3K and Grb2 (Taniguchi *et al*., 2006) (**Figure 4**).

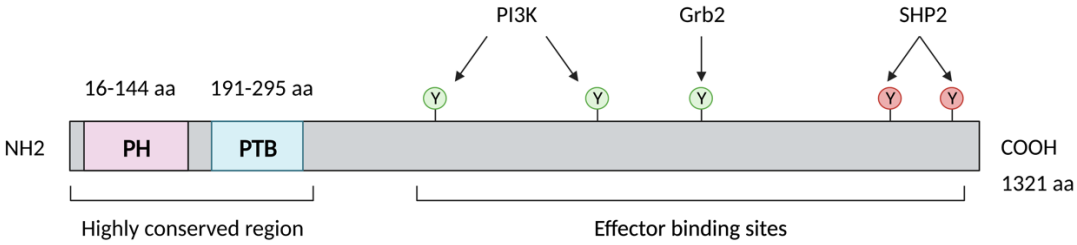

FIGURE 4. Schematic representation of the IRS2 protein. Aa, aminoacid; Grb2, growth factor receptor-bound protein 2; PH, pleckstrin homology domain; PI3K, phosphatidylinositol 3-kinase; PTB, phosphotyrosine binding domain; SHP2, SH2-containing protein tyrosine phosphatase 2; Y, phosphotyrosine residues. *Modified from Taniguchi et al., 2006. Generated using Biorender.*

The various domains present in IRS2 play a crucial role in enabling the protein to effectively exert its function. Notably, IRS2 is recruited to sites of tyrosine kinase activation, in close contact with IR and IGF1R, owing to the presence of both its PH and PTB domains. The PH domain binds to specific phospholipid second messengers, phosphatidylinositol-3, 4, 5-phosphate (PIP_3), while the PTB domain regulates the direct protein-protein interaction of IRS2 with activated IR or IGF1R, specifically phosphorylated at NPXY motifs (Brummer *et al*., 2010).

Upon association with activated tyrosine kinase receptor IR or IGF1R, IRS2 is phosphorylated on multiple tyrosine residues, leading to the recruitment of specific SH2-containing effector proteins, specifically the adaptor molecule Grb2 and the p85 regulatory subunit of PI3K. In turn, Grb2 associates with son-of-sevenless (SOS) to activate the Ras-MAPK pathway, while the p110 catalytic subunit of PI3K generates PIP_3, which leads to the activation of the serine/threonine kinase AKT. Consequently, they regulate mitogenic and metabolic functions by promoting gene expression for cellular proliferation, survival, differentiation, regulation of metabolism and general growth (Taniguchi *et al*., 2006; Mardilovich *et al*., 2009) (**Figure 5**).

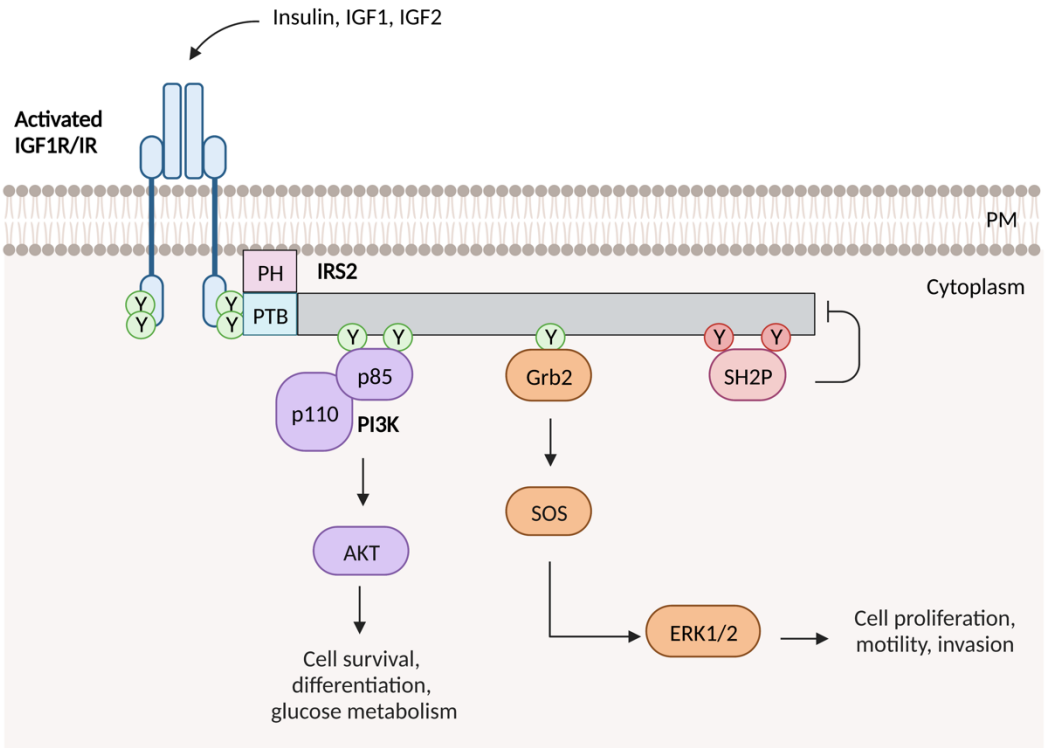

FIGURE 5. Signaling pathways activated through the IRS2 docking protein. Upon ligand binding (insulin, insuline-like growth factor (IGF) 1 or 2), tyrosine kinase insulin receptor (IR) or insuline-like growth factor 1 receptor (IGF1R) dimers suffer a cross-phosphorylation of their cytoplasmic tail, resulting in phosphotyrosine residues (Y). IRS2 is recruited to the activated IGF1R or IR by direct contact with the plasma membrane (PM) through its pleckstrin homology (PH) domain and by contact with the Y through its phosphotyrosine binding (PTB) domain. Then, it is phosphorylated in its tyrosine residues. Finally, effector proteins containing an SH2 domain (p85 regulatory subunit of phosphatidylinositol 3-kinase (PI3K) and growth factor receptor-bound protein 2 (Grb2)) bind to this docking protein and transduce the signal to AKT and son-of-sevenless (SOS), respectively. In turn, MAPK cascade (in orange) and PI3K/AKT (in purple) activate gene expression for cell survival, proliferation, differentiation and metabolism. An inhibitory mechanism is exerted by the SH2-containing protein tyrosine phosphatase 2 (SH2P), which dephosphorylates the phosphotyrosines involved in the binding of PI3K and Grb2. *Modified from Mardilovich et al., 2009. Generated using Biorender.*

1.2.1.2. Components involved in the insulin/IGF system

The insulin/IGF system is composed of various components, including three ligands (insulin, IGF1 and IGF2), four transmembrane receptors (IR, IGF1R, IGF2R and hybrid IR-IGF1R) and six IGF binding proteins (IGFBPs 1-6) that transport IGFs in the circulation, prolonging their half-life (Randhawa and Cohen, 2005). The peptide hormones insulin, IGF1 and IGF2 mediate a variety of previously-mentioned metabolic and mitogenic effects, by binding to and activating their specific receptor tyrosine kinases. Generally, insulin binds to IR, while IGF1 and IGF2 bind to IGF1R to exert their functions (Hiden *et al*., 2009).

IR and IGF1R belong to a subfamily of receptor tyrosine kinases. These receptors are heterotetrameric transmembrane glycoproteins composed of two extracellular α-subunits and two transmembrane ß-subunits. Two of the α-ß dimers are linked with disulfide bonds to form the tetramer, making it also possible to construct a hybrid IR-IGF1R complex (Taniguchi *et al*., 2006).

However, IGF2R, also known as the cation-independent mannose 6 phosphate receptor, is structurally unrelated to either IGF1R or IR. It only has one polypeptide chain, which is primarily extracytoplasmic and lacks tyrosine kinase activity (Harris and Westwood, 2012). Thus, it has no site to which IRS2 can bind to, and it only functions as a clearance receptor, modulating the bioavailability of IGF2 (Harris *et al*., 2011) by internalizing it and targeting it for lysosomal degradation (Forbes *et al*., 2020).

Due to the considerable structural homology between the IR and the IGF1R, insulin and IGFs can bind to various receptors with distinct affinity (**Figure 6**). At physiological concentrations, insulin and IGF1 bind to their own receptors, IR and IGF1R respectively, but also to the hybrid IR-IGF1R with less affinity (Randhawa and Cohen, 2005). Conversely, IGF2 binds to the IGF1R and, in a lesser amount to the isoform A of IR (IR_A) lacking exon 11, and to IGF2R (Harris and Westwood, 2012).

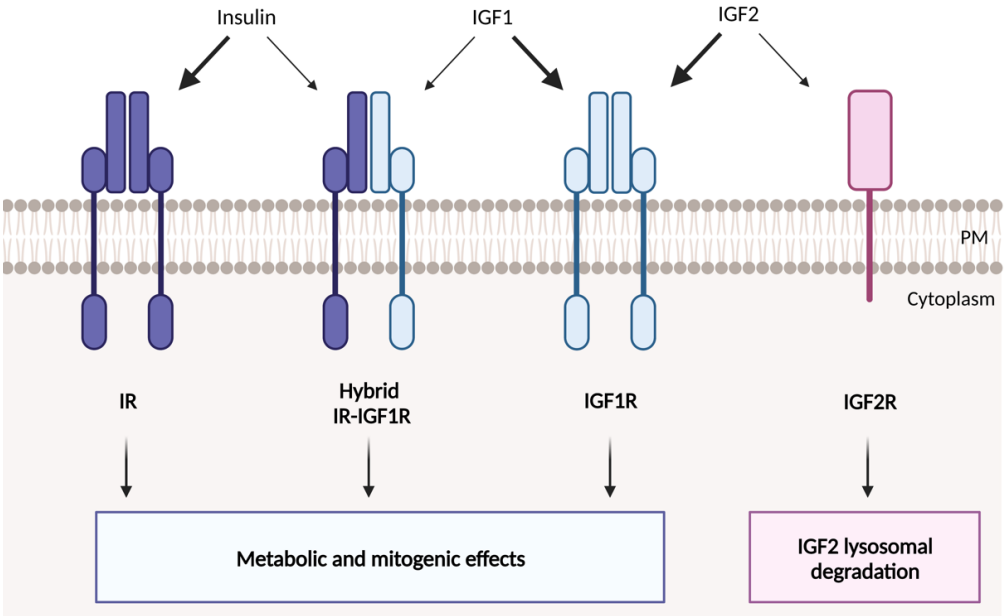

FIGURE 6. Ligand binding affinity for each receptor involved in the insulin/IGF system. Arrow intensity is proportional to the binding affinity, a thicker arrow indicates more affinity for a certain receptor than a thinner one. IGF1, insulin-like growth factor 1; IGF2, insulin-like growth factor 2; IGF1R, insulin-like growth factor 1 receptor; IGF2R, insulin-like growth factor 2 receptor; IR, insulin receptor; PM, plasma membrane. *Modified from Randhawa and Cohen, 2005; Harris and Westwood, 2012. Generated using Biorender.*

1.2.2. Placental defects related to IRS2 and the insulin/IGF axis

Knockout (KO) mouse models have provided tremendous insight into the diverse functions of genes, as well as their roles in diseases. In this regard, the study of mice lacking *Irs2* has shown that dysfunction of IRS2 may contribute to the pathophysiology of human type 2 diabetes by impairing peripheral insulin signaling and pancreatic ß-cell function (Withers *et al*., 1998; Oliveira *et al*., 2014). *Irs2* KO male adult mice died of dehydration and hyperosmolar coma. Female KO mice survived, but they developed diabetes type 2. Intriguingly, the pups of the KO litters showed a 10% decrease in size compared to control counterparts (wild types, WT), which may be indicative of placental insufficiency. Posterior studies showed that this deletion causes female infertility and reduction in ovary size, which together with evidence from in *Drosophila* and *C. elegans*, indicates a conserved mechanism for integrating reproduction and metabolism (Burks *et al*., 2000).

Moreover, knocking out other components of the IGF axis, like IGF1 and IGF2 have reported that this signaling system is essential for fetal development and growth (Forbes *et al*., 2020). IGF2, which is highly expressed in the placenta (Sferruzzi-Perri, 2018), may influence fetal growth by promoting normal placental development and function. This was seen in placental specific *Igf2* KO studies, where deletion of this gene resulted in reduced growth of the placenta (Constância *et al*., 2002), decreased amino acid transfer (Sferruzzi-Perri *et al*., 2011a), and consequently fetal growth restriction (FGR). Similar preliminary results from our laboratory showed a slower proliferation rate in mTSCs lacking IRS2 that WT control cells.

Furthermore, recent studies (Sandovici *et al*., 2022) highlight that fetus-derived IGF2 controls the growth and differentiation of trophoblast cells, supporting their normal development, particularly of the SynT-II layer of the placental labyrinth. Intriguingly, preliminary RT-qPCR analysis results from our laboratory show that IRS2 expression in E15.5 placentas is higher in the labyrinth, compared to the junctional zone. This region is essential for nutrient transport, thereby indicating a possible function of the IRS2 docking protein downstream of IGF2, related to resource allocation during gestation.

Thus, an impaired insulin/IGF signaling pathway mediated by IRS2 could lead to FGR and abnormalities in nutrient supply. In turn, this results in disruptions of fetal organ development, showing life-long consequences in the offspring, such as cardiovascular and metabolic dysfunction (Sferruzzi-Perri, 2018).

2. OBJECTIVES

The hypothesis underlying the experimental design is that IRS2 has an important role on early placental development and resource allocation to the fetus, by the integration of IGF signals. The main objective of this work is to decipher the molecular function of IRS2 in the placentation molecular mechanisms through a study of mouse trophoblast stem cells (mTSCs).

Specific objectives include:

1. Analyzing the dynamics of IRS2 expression during trophoblast differentiation.
2. Comparing the transcriptome of *Irs2* KO and control mTSCs.
3. Delineating the signaling pathways mediated by IRS2 in trophoblast stem cells (through IGF1 and IGF2 stimulation).

3. MATERIALS AND METHODS

3.1. CRISPR/Cas9 knockout of *Irs2* in mouse trophoblast stem cells

To obtain mouse trophoblast stem cell lines lacking IRS2, clonal knockout *Irs2* mTSCs were previously generated in the laboratory by employing the CRISPR/Cas9 gene editing technology. For this purpose, the commercial vector LV01 (SigmaAldrich, S0187) was used (**Figure 7A**). This plasmid contains the Cas9 nuclease and the guide RNA (gRNA) composed of the CRISPR RNA (crRNA) and the trans-activating CRISPR RNA (tracrRNA). The crRNA, corresponding to 5'-CGGAGGCACTACCGCTGGA-3', is complementary to the target sequence in the *Irs2* exon 1 coding region (**Figure 7B**). For the wild type controls, the non-targeting (NT) PX458 (pSpCas9(BB)-2A-GFP) plasmid (Addgene, plasmid #48138) was employed, containing a scrambled gRNA, which does not match any specific target in the genome of interest.

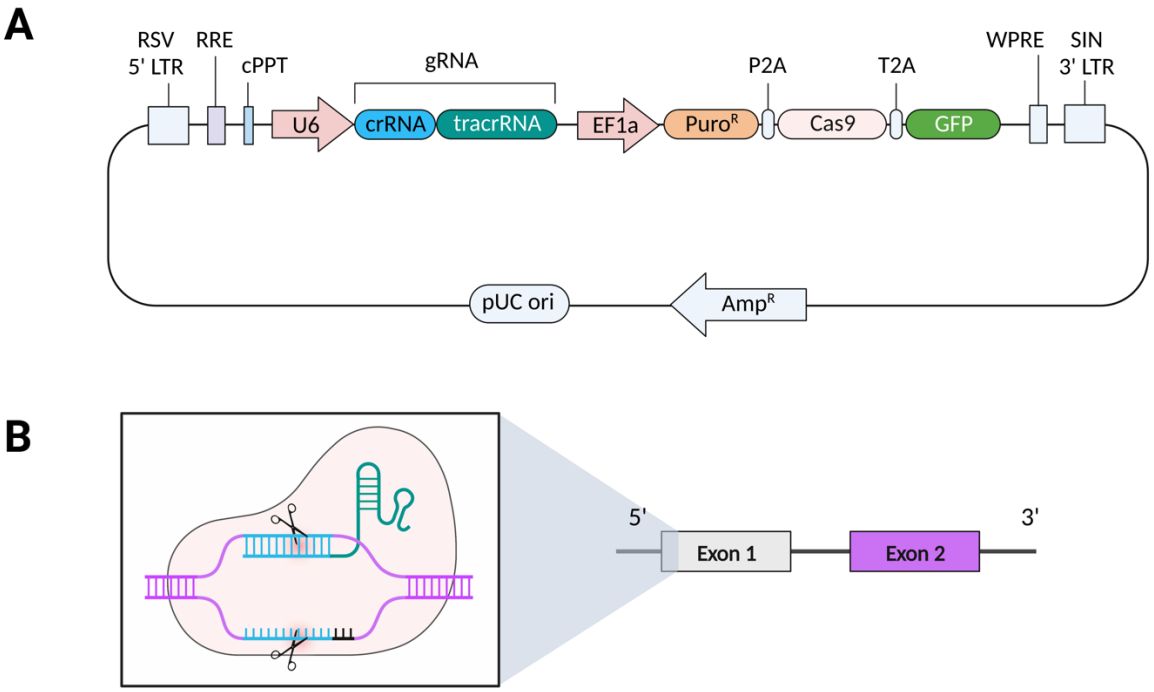

FIGURE 7. CRISPR/Cas9 technology to knock out Irs2 in mouse trophoblast stem cells. **(A)** Schematic representation of the LV01 (U6-gRNA:EF1a-puro-2A-Cas9-2A-tGFP) plasmid from SigmaAldrich. **(B)** CRISPR RNA (crRNA) of guide RNA (gRNA) targets a sequence of *Irs2* in the coding region of exon 1. *Generated using Biorender.*

Supercompetent XL1-Blue *E. coli* strain (Agilent, 200236) was transformed with the LV01 plasmid and the control NT PX458 plasmid. The colonies that had uptaken the plasmid were selected in LB plates containing ampicillin (100 µg/mL), since they express the resistance gene for this antibiotic. Then, the plasmid DNA was extracted from cultures using the QIAprep Spin Miniprep Kit PK/250 (QIAGEN, 27106) and it was sequenced to validate that the gRNA remained intact. Transfection of mTSCs was performed using Lipofectamine 2000 (ThermoFisher Scientific, 11668019).

Clonal cell lines were generated using fluorescence activated cell sorting (FACS), where transfected GFP$^+$ cells were sorted at single cell level into each well of a 96-well plate. Clonal KO verification was accomplished by extracting DNA, performing a PCR, running an agarose gel and sequencing the samples by Sanger. Finally, it was confirmed that 4 different clones were lacking *Irs2* (KO1, KO2, KO7, KO8) (**Figure 8**).

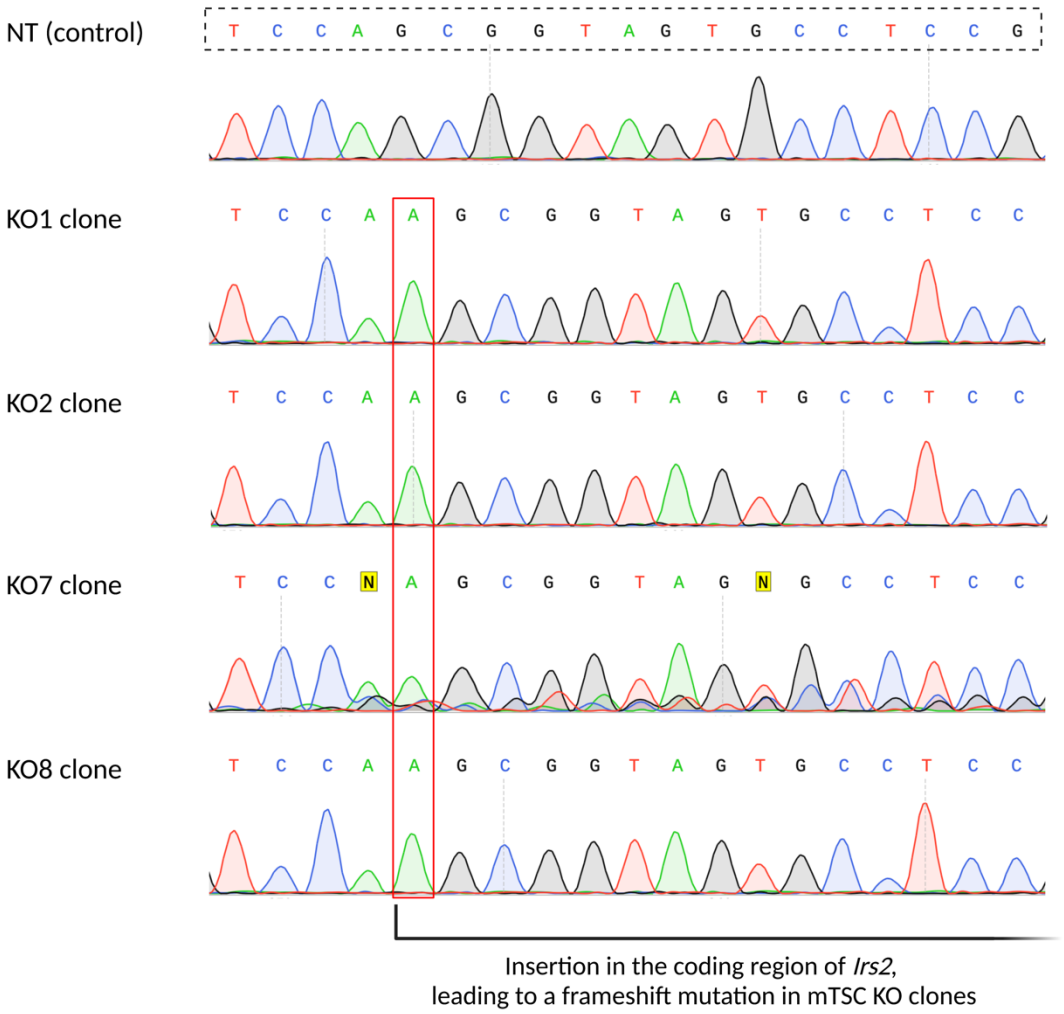

FIGURE 8. Sanger sequencing chromatograms after CRISPR/Cas9. Comparison of non-targeting (NT) control clone with knockout clones (KO1, KO2, KO7, KO8) for their validation. Dashed-line rectangle indicates the target sequence in the coding region of the exon 1 of *Irs2* (5'-TCCAGCGGTAGTGCCTCCG-3'), which is complementary to the crRNA of the gRNA (5'-CGGAGGCACTACCGCTGGA-3'). Red-line rectangle highlights an adenine (A) insertion, leading to frameshift mutations in the coding region of *Irs2*. This confirms that there has been an effective and specific double stranded DNA break caused by the Cas9 nuclease, which the KO clones have repaired by non-homologous end joining (NHEJ), resulting in insertions and deletions (InDels). *Preliminary data from the laboratory.*

Furthermore, depletion of IRS2 at the protein level was also confirmed in the *Irs2* KO clones (KO1, KO2, KO7 and KO8) by carrying out a Western Blot analysis of NT and KO mTSC clones cultured in complete medium (**Figure 9**).

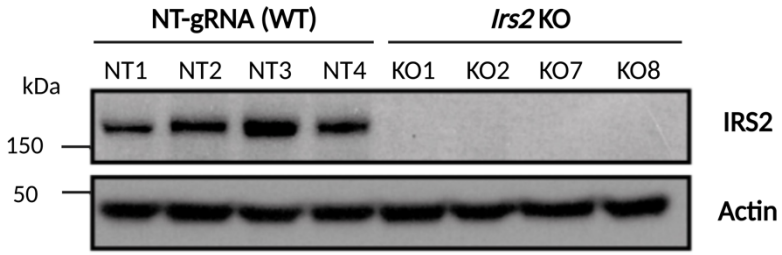

FIGURE 9. Western Blot for IRS2 on mTSCs confirming an effective depletion of the protein in KO clones. NT1, NT2, NT3 and NT4 are control (non-targeting guide RNA, NT-gRNA) wild type (WT) clones. KO1, KO2, KO7 and KO8 are *Irs2* knockout (KO) clones. Actin was used as internal control for protein loading. *Preliminary data from the laboratory.*

3.2. Cell culture

TS-Rs26 mouse trophoblast stem cells (mTSCs) were cultured in different culture mediums (**Table 1**) at 37°C and 5% CO_2. Complete and base mediums were used in the differentiation experiments, while complete, starving and stimulation mediums were used in the stimulation experiments.

TABLE 1. Components of the different culture mediums used in the experiments.

Base medium	Complete medium	Starving medium	Stimulation mediums
20% FBS (Gibco, 10270)	70% MEFs-conditioned medium	RPMI 1640 (Lonza™ BioWhittacker™, BE12-115F)	RPMI 1640 (Lonza™ BioWhittacker™, BE12-115F)
RPMI 1640 (Lonza™ BioWhittacker™, BE12-115F)	30% base medium	Anti-Anti 100X (Gibco, 15240-062)	Anti-Anti 100X (Gibco, 15240-062)
Anti-Anti 100X (Gibco, 15240-062)	FGF 1000X (Sigma, F0291)	Sodium Pyruvate 100 mM 100X (Gibco, 11360-039)	Sodium Pyruvate 100 mM 100X (Gibco, 11360-039)
Sodium Pyruvate 100 mM 100X (Gibco, 11360-039)	Heparin 1000X (Sigma-Aldrich, H3149-10KU)	ß-mercaptoethanol 50 mM 1000X (Gibco, 31350-010)	ß-mercaptoethanol 50 mM 1000X (Gibco, 31350-010)
ß-mercaptoethanol 50 mM 1000X (Gibco, 31350-010)			50 ng/mL IGF2 (R&D Systems, 792-MG-050) or 100 ng/mL IGF1 (STEMCELL Technologies, 78022.1)

Before reaching confluency, passages were done every 2 to 3 days to avoid trophoblast differentiation and maintain their autorenewal capacity. In order to pass the cells, they were washed and detached from the plate surface. Washing was done by removing the medium of each plate and adding PBS (HyClone, SH30028.03), which was later discarded. Detachment of the cells was attained by adding 400 µL of 0,25% Trypsin-EDTA 1X (Gibco, 25200-056) and incubating them for 5 minutes at 37°C. Then, trypsin action was stopped with base medium. Finally, cells were centrifuged at 300 g during 3 min, resuspended in complete medium and seeded in a new culture plate, with its corresponding dilution.

3.2.1. 6-day time course trophoblast differentiation experiments

3 mTSC *Irs2* NT and 3 mTSC *Irs2* KO clones were thawed and grown in 60 mm culture plates using complete medium at 37°C and 5% CO_2. After 2 days in exponential growth, the cells were seeded into 7 plates per clone, one for each day of trophoblast differentiation (D0-D6) (**Figure 10**). While complete medium was used for the D0 plates, base medium was employed for D1-D6 plates, in order to promote differentiation of the mTSCs. Cells were collected every day by removing the medium from the plates corresponding to that differentiation day, washed twice with PBS and stored at -80°C until posterior protein extraction.

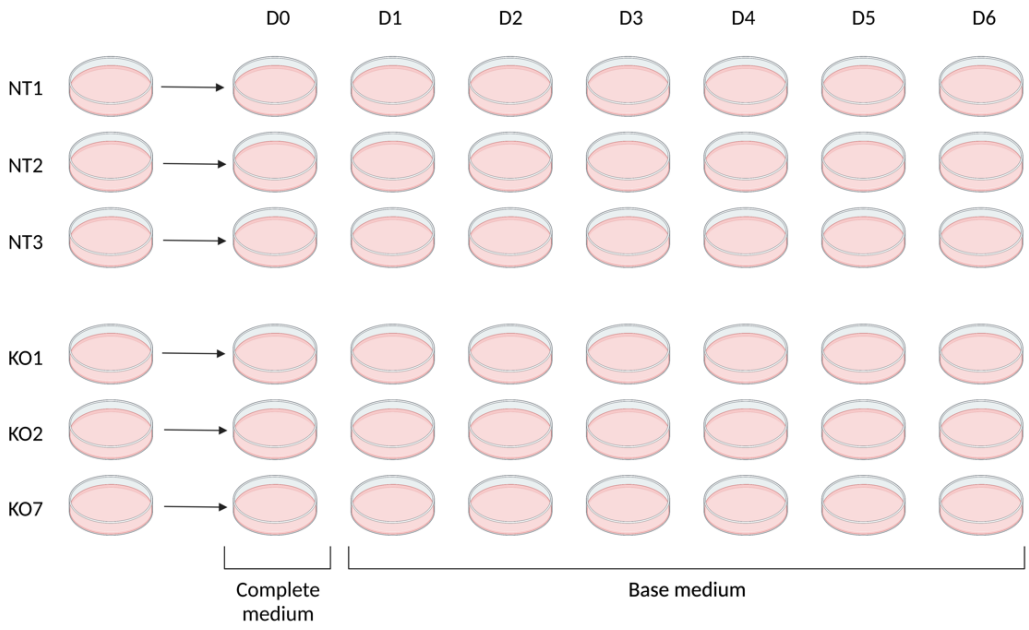

FIGURE 10. Schematic representation of the cultured plates for the trophoblast differentiation experiment from day 0 to day 6. Three control (NT) and three knockout (KO) *Irs2* mTSC clones were cultured in complete medium for day 0 of trophoblast differentiation (D0) and base medium for day 1 (D1) until day 6 (D6) of differentiation. *Generated using Biorender.*

3.2.2. Stimulation experiments with IGF2 and IGF1

For IGF2 stimulation, 3 mTSC *Irs2* NT and 3 mTSC *Irs2* KO clones were thawed and cultured in 60 mm culture plates using complete medium at 37°C and 5% CO_2. After 2 days of exponential growth, the cells were seeded into 4 plates per clone, one for each stimulation time (0 minutes, 5 minutes, 10 minutes, and 30 minutes) (**Figure 11A**). This time frame was chosen with the aim of covering the early signaling response of IGFs stimulation.

The following day, the complete medium was discarded and cells were washed twice with PBS. Then, they were arrested using starving medium lacking FBS, FGF/heparin and conditioned medium, which serves to synchronize the cells at the same metabolism state. After 8 hours of starvation, stimulation was carried out. Starving medium was substituted with stimulation medium containing IGF2 (50 ng/mL) for the 5-minute (5´), the 10-minute (10´) and the 30-minute (30´) plates. Then, after their corresponding time, the stimulation medium was removed, the plates were washed twice with PBS and they were stored at -80ºC until the protein extraction protocol was performed. The same steps were followed for IGF1 stimulation, but the stimulation dose was different (100 ng/mL).

Moreover, to do posterior immunofluorescence (IF) analysis, 1 mTSC *Irs2* NT and 1 mTSC *Irs2* KO clones were seeded in triplicates on round glass coverslips in a 24-well plate (**Figure 11B**). The same stimulation procedure was followed and finally, washed cells were fixed using paraformaldehyde (PFA) 4X (Electron Microscopy Sciences, 15710). They were stored at 4ºC until the IF staining.

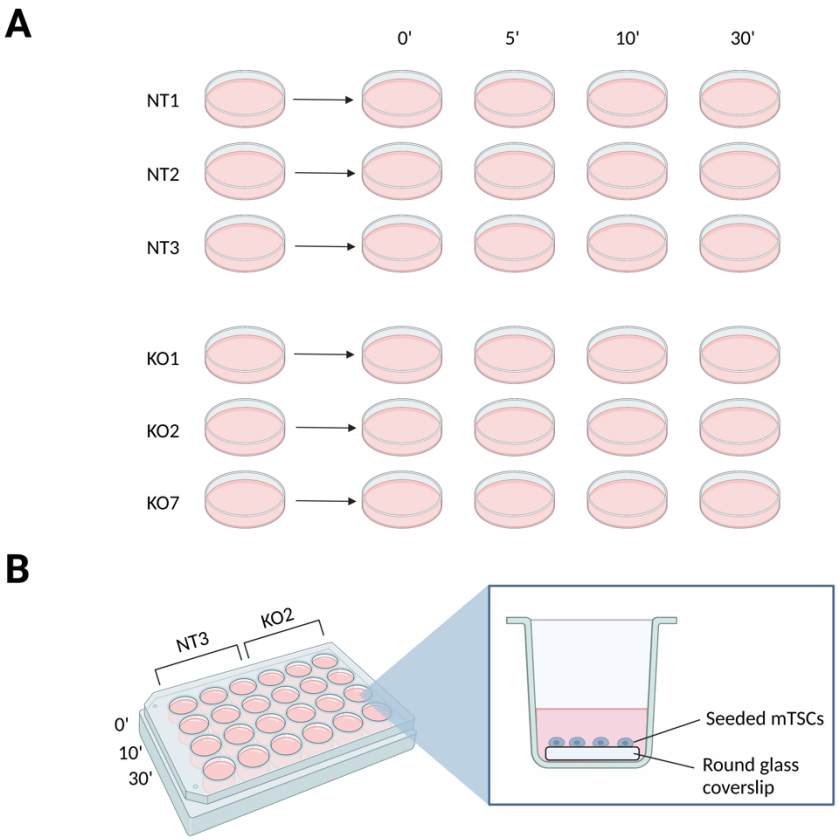

FIGURE 11. Schematic representation of the cultured plates for the stimulation experiments. **(A)** Three control (NT) and three knockout (KO) *Irs2* mTSC clones were arrested by culturing them in starving medium during 8 hours. Then, they were stimulated with IGF2 (50 ng/mL) or with IGF1 (100 ng/mL) during 5 minutes (5'), 10 minutes (10') and 30 (30') minutes. **(B)** Preparation of IGF2-stimulated cells for immunofluorescence staining. One control (NT3) and one knockout (KO2) *Irs2* mTSC clones were seeded in triplicates on round glass coverslips, arrested with starving medium and 8 hours after stimulated with IGF2 (50 ng/mL) for 0, 10 and 30 minutes. *Generated using Biorender.*

3.3. Western Blot (WB)

3.3.1. Protein extraction and quantification

mTSCs of the previously explained trophoblast differentiation and stimulation experiments were analyzed by Western Blot (WB), for which protein extraction and quantification was needed. To avoid protein degradation, the whole protein extraction protocol was performed keeping the plates in contact with ice. Cells were lysed, detached of each plate surface, collected in a 1,5-mL Eppendorf tube and kept in ice. For this purpose, 200 µL of lysis buffer (cOmplete™ Protease Inhibitor Cocktail (Roche, 11697498001) and triplex buffer (50 mM TRIS-HCl pH 8, 120 mM NaCl, 0,1% SDS, NONIDER P-40, 0,5% DOC, distilled water)) were added and a scraper was used to mechanically detach the cells. The cells were incubated at 4ºC for 30 minutes, and were vortexed every 10 minutes. Lastly, 4ºC centrifugation was done at maximum speed (16.100 g) during 10 min and the supernatant was transferred to new Eppendorf tubes.

Afterwards, protein quantification was done to estimate the volume of each sample needed to load 40 µg in the posterior SDS-PAGE. The Pierce™ BCA Protein Assay Kit (ThermoScientific, 23227) procedure was carried out using a 96-well plate. This plate was incubated at 37ºC for 30 minutes and then the absorbance was read with the VICTOR2™ PerkinElmer spectrophotometer. A standard curve was represented from different known concentrations of bovine serum albumin (BSA) and their absorbances. Based on this curve, the protein concentration of each sample was extrapolated.

3.3.2. SDS-polyacrylamide gel electrophoresis (SDS-PAGE)

SDS-polyacrylamide gels were prepared at 4% acrylamide (Bio-Rad, 1610149) for the stacking gel and 7% for the separating gel (percentage based on the molecular weight of the studied proteins). The stacking and separating gels also differ in the buffer pH, being lower the former (6,8) than the latter (8,8). This acidic environment and lower acrylamide concentrations contribute to the concentration of the sample in the stacking gel, while the resolving gel separates the proteins based on their molecular weight.

30-µL loading samples were produced by mixing in a 1,5-mL Eppendorf tube each protein extract (volume corresponding to 40 ng of protein content) with 4X loading buffer (20 mM TRIS-HCl pH6,8, 40% glycerol 87% purity, 8% SDS, bromophenol blue and 1 M DTT). The Eppendorf tubes were incubated at 95ºC for 5 minutes in the ThermoShaker, time during which the proteins were denaturated due to heat and the presence of sodium dodecyl-sulfate (SDS) and reducing agent dithiotheitrol (DTT). SDS introduces negative charges to the amino acids, resulting in the disruption of the secondary and tertiary protein structure. Heat facilitates the binding of SDS to hydrophobic regions, leading to complete denaturation, and DTT reduces disulfide bonds.

Finally, the 30-µL samples were loaded into the SDS-PAGE gel. In the first well, 5 µL of the PageRuler Prestained Protein Ladder (ThermoFisher Scientific, 26616) molecular weight marker were charged. Once loaded and submerged in electrophoresis buffer (glycine (Fisher bioreagents, BP381-1), Tris Base (Fisher bioreagents, BP152-1), 10% SDS (Fisher bioreagents, BP166-500) and miliQ water), the electrophoresis was run at 100 V until the samples overpassed the stacking gel, moment in which the voltage was increased to 140 V. It was left running until the bands of the marker corresponding to molecular weight of the proteins of interest were correctly resolved.

3.3.3. Electrotransfer and detection

After SPS-PAGE, proteins were transferred from the gel to a previously activated Immobilon-P polyvinylidene difluoride (PVDF) membrane (Merck, IPVH00010). The activation of the membrane was done by submerging it in methanol (Fisher bioreagents, BP1105-4) for 3 minutes, then washing it with type II water and finally immersing it in TBS-T 1X (Tris Base, NaCl (VWR chemicals, 27810.295), Tween® 20 (Sigma-Aldrich, P1379) and miliQ water). The electrotransfer was performed at 290 mA for 90 minutes with transfer buffer (glycine, Tris Base, methanol and miliQ water) in ice. Then, the membrane was stained with Ponceau red (Sigma-Aldrich, P3504) to check that the proteins had correctly transferred. Ponceau was then removed with type II water and the membranes were placed in TBT-T 1X. While the bands could still be seen before the whole Ponceau was fully destained, the membrane was cut into different pieces corresponding to the molecular weight of each protein of interest.

Blocking was then carried out, in which the non-specific sites were blocked by incubating the membranes for 1 hour at room temperature (RT) with 5% milk in TBS-T 1X or, in the case of phosphorylated proteins, 5% BSA (Sigma-Aldrich, A7906-100G) in TBS-T 1X. After blocking, the membranes were incubated overnight at at 4^{o}C with the corresponding primary antibody (**Table 2**) diluted 1:3000 in blocking solution (5% milk in TBS-T 1X). The following day, the membranes were washed with TBS-T 1X during 5 minutes thrice and then incubated with the secondary antibodies (**Table 3**) for 1 hour at RT. These antibodies are conjugated to the horse radish peroxidase (HRP) enzyme and diluted 1:3000 in blocking solution. Finally, the membranes were thoroughly washed and ready for posterior revealing.

To reveal, the membranes were firstly covered during 1 minute with Enhanced Chemiluminescence (ECL) (Amersham, RPN2106), which is a luminol-based substrate for HRP. Next, they were placed in the developing cassette, in which they were taken to the darkroom. There, they were exposed to an autoradiographic film (Agfa, CP-BU M) which captures the light emitted from the HRP-ECL chemical reaction. The film was placed inside the cassette during different times, until the optimal interval was found. They were finally revealed employing the Agfa-Gevaert Curix 60 system, which has three different solutions to develop the films: developer, water and fixer.

TABLE 2. Primary antibodies used for the WB detection.

Primary antibody	Species	Molecular weight (kDa)	Reference
AKT	Rabbit	60	9272D, Cell Signaling Technology
ERK	Rabbit	42/44	9102S, Cell Signaling Technology
HSP90	Rabbit	90	4877S, Cell Signaling Technology
IRS2	Mouse	185	MABS15, SigmaAldrich
pAKT (S473)	Rabbit	60	9271S, Cell Signaling Technology
pERK (p42/44)	Mouse	42/44	9106L, Cell Signaling Technology

TABLE 3. Secondary antibodies used for the WB detection.

Secondary antibody	Species	Reference
Anti-mouse IgG	Goat	1706516, BIO-RAD
Anti-rabbit IgG	Goat	1706515, BIO-RAD

3.4. Immunofluorescence (IF) staining

Six rounded glass coverslips of IGF2-stimulated cells (1 mTSC *Irs2* NT and 1 mTSC *Irs2* KO clones at times 0, 10 and 30 minutes of IGF2 stimulation) were used for pAKT immunofluorescence (IF) staining. Cells were permeabilized with PBS, 0,3% Triton X-100 (Fisher bioreagents, BP151-100) for 10 minutes to facilitate antibodies crossing the cell membrane. They were then blocked to avoid non-specific signals with IF blocking solution (PBS, 0,1% Tween® 20, 1% BSA) for 1 hour at RT. Primary antibody anti-pAKT diluted 1:100 in blocking solution (**Table 4**) was applied overnight at 4°C in a humid chamber.

The next day, after washing with PBS and IF blocking solution, secondary antibody diluted 1:400 in blocking solution (**Table 4**) was incubated in darkness for 1 hour at RT. It is marked with the Alexa488 fluorochrome, making it essential to protect the coverslips from the light. Coverslips were further washed and incubated for 5 minutes with DAPI (Roche, 10236276001) diluted 1:1000 in PBS. Finally, coverslips were mounted on slides using VECTASHIELD® mounting medium for fluorescence (Vector Laboratories, H-1000) and kept at 4°C until imaging with fluorescent microscopy.

TABLE 4. Primary and secondary antibodies used for the IF staining.

		Species	Dilution	Reference
Primary antibody	**pAKT**	Rabbit	1:100	9271S, Cell Signaling Technology
Secondary antibody	**Alexa488**	Goat anti-rabbit	1:400	A11008, ThermoFisher Scientific

3.5. Image processing

The Western Blot films were scanned and the band intensities were quantified using ImageJ (ImageJ Software, National Institutes of Health, Bethesda, MD, USA). Immunofluorescence samples were visualized using the Leica DMi8, and 5 images were obtained per condition (*Irs2* KO and NT) and per time of IGF2 stimulation (0, 5, 10, 30 minutes). These images were quantified with the ImageJ software and then analyzed and processed employing Photoshop (Adobe Photoshop Software, Adobe Inc., San Jose, CA, USA).

3.6. Statistical analysis

All the graphs, calculations and statistical analyses were performed using GraphPad Prism (GraphPad Software, San Diego, CA, USA). Data were considered normally distributed and analyzed using ordinary one-way ANOVA or two-way ANOVA when appropriate, followed by the Dunnett's or Šídák's post-hoc test for multiple comparisons, respectively. Data are shown as the mean ± SEM (standard error of mean). For *p*-values < 0,05, differences were regarded as statistically significant.

3.7. RNA-seq

Transcriptomic data were previously obtained in the laboratory by performing RNA-seq. Total RNA was extracted from 4 mTSC *Irs2* NT and 4 mTSC *Irs2* KO clones at day 0 (D0), 3 (D3) and 6 (D6) of trophoblast differentiation, by using TRIZol reagent (ThermoFisher Scientific, 15596026) and the TURBO DNA-free kit (Life Technologies, AM1970). Then, by following the dUTP method using the stranded mRNA LT sample kit (Illumina), adapter indexed strand-specific RNA-seq libraries for NT and *Irs2* KO mTSCs were generated from 1 µg of total RNA. Finally, libraries were pooled and loaded onto the Illumina NovaSeq 6000 system. For deep sequencing, the libraries were sequenced with 150 bp paired-end reads. FASTQ files were aligned to the *Mus musculus* GRCm39 reference genome using HISAT2 v2.1.0.

3.8. Bioinformatic analysis

Transcriptomic data from trophoblast differentiation of *Irs2*-mutant mTSCs compared to wild types was analyzed. The trimmed BAM files previously obtained in the laboratory were quantitated by using the RNA-seq quantitation pipeline in SeqMonk (Babraham Bioinformatics Group) and normalized according to total number of mapped reads and gene length (fragments per kilo base of transcript per million mapped reads, FPKM).

Differentially expressed genes (DEGs) were calculated using DESeq2 and FPKM Fold Change ≥ 2 with *p*-value < 0,05 and adjusted for multiple test correction using the Benjamini-Hochberg method. For more stringency, DESeq2 analysis was combined with intensity difference filters in SeqMonk. Heatmaps and principal component analysis (PCA) plots were obtained using SeqMonk. Finally, pathway enrichment analysis was carried out in Database for Annotation, Visualization and Integrated Discovery (DAVID). Gene ontology (GO) terms with *p*-value < 0,05 were considered significant.

4. RESULTS AND DISCUSSION

4.1. *Irs2* is expressed in trophoblast stem cell conditions and modulated throughout trophoblast differentiation

To gain insight into the role of *Irs2* in trophoblast development, we firstly examined the dynamics of its expression in a 6-day time course differentiation experiment of mTSCs in which we analyzed the IRS2 protein level. The expression profile of *Irs2* demonstrated that it is highly expressed in trophoblast stem cell conditions, showing a modulation along differentiation (**Figure 12A**). An increase in IRS2 levels was observed at around day 4 of trophoblast differentiation (D4) until D6. This time frame corresponds to the final differentiation of TGCs (Pérez-García *et al*., 2018), suggesting that IRS2 may be implicated in trophoblast development, more specifically, as will be discussed further, in the differentiation towards sinusoidal TGCs.

To elucidate the mechanism of regulation of Irs2 expression, we analyzed the transcriptomic data previously obtained in the laboratory to determine whether it occurs at the pre- or post-transcriptional level. Further corroborating WB results, the heatmap of *Irs2* at day 0, 3 and 6 of trophoblast differentiation confirmed an upregulation of the *Irs2* mRNA levels at D6 with regards to D0 and D3 (**Figure 12B**). This modulation in the mRNA levels indicates that it is transcriptionally regulated. However, further studies are required to determine the specific mechanisms governing this change in expression.

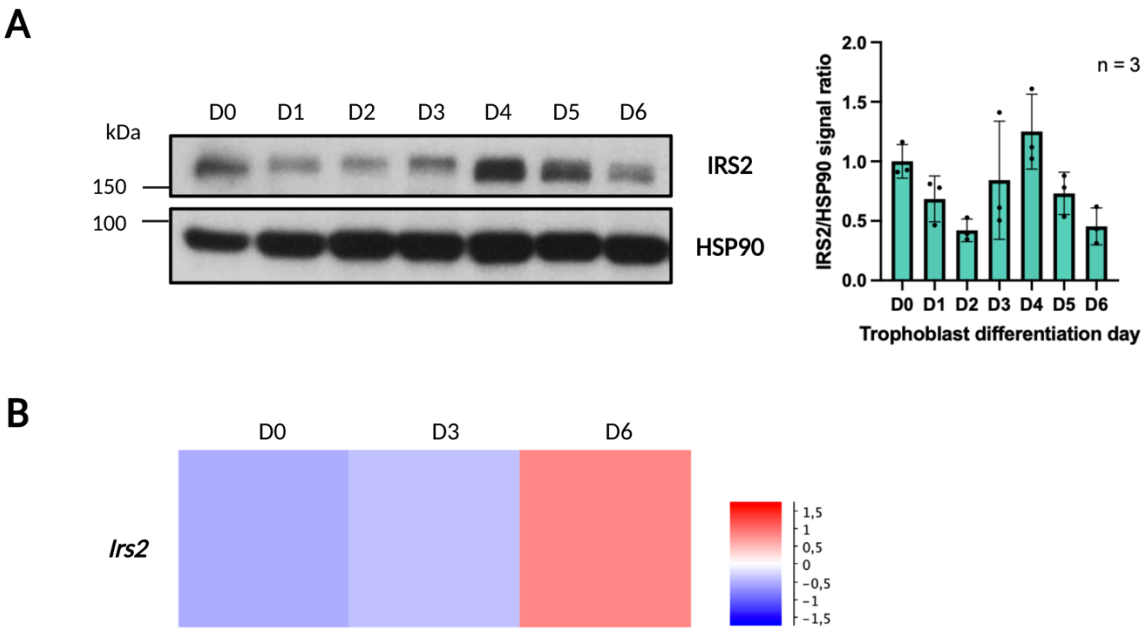

FIGURE 12. Irs2 expression is modulated during trophoblast differentiation. **(A)** Western Blot for IRS2 on mTSCs in the stem cell state (D0) and upon differentiation (D1-D6). Quantification of band intensities of three independent experiments is shown in the right-hand-side graph. Data are normalized against HSP90 and represented relative to stem cell conditions (D0); mean ± SEM (one-way ANOVA with Dunnett's multiple comparisons test). **(B)** Heatmap of *Irs2* expression in mTSCs in stem cell conditions (D0) and day 3 (D3) and 6 (D6) of differentiation. Four independent biological replicates per genotype were sequenced.

4.2. IRS2 depletion affects trophoblast differentiation towards sinusoidal TGCs, the subpopulation of invasive cells located in the labyrinth

To further investigate the effect of IRS2 on trophoblast differentiation, we studied the global expression profile of *Irs2*-null mTSCs (KO) compared to control cells (NT) in stem cell conditions (D0) and upon 3 and 6 days of differentiation (D3 and D6). Unbiased clustering and principal component analysis (PCA) demonstrated that the differentially expressed genes (DEGs) were mostly determined by the day of differentiation, rather than by the absence of IRS2 (**Figure 13A**). However, at D6, IRS2 depletion seemed to have a higher effect, suggesting that there is an impact on late differentiation events for mouse trophoblast stem cells with IRS2 deficiency.

To continue exploring the role of IRS2 in late trophoblast differentiation, we performed a stringent assessment of the DEGs (DESeq2 and intensity difference filter), comparing the transcriptome at day 6 (D6) of *Irs2* KO clones with controls. The analysis revealed a total of 32 genes significantly deregulated in D6, with a downregulation of genes involved in sinusoidal trophoblast giant cell (TGC) development (*Ctsq*, *Ctsr*, *Ctsj)* and vascularization (*Prl2c5*, *Nos2*) for cells lacking IRS2 (**Figure 13B**). In line with these observations, gene ontology analysis revealed an overrepresentation of cell differentiation, peptidase activity and binding to actin and extracellular matrix proteins, such as fibronectin and collagen (**Figure 13C**).

Ctsq, *Ctsr* and *Ctsj* are genes encoding for Cathepsins Q, R and J, respectively. They are highly expressed in the labyrinth by sinusoidal TGCs (Mason, 2008), and, as previously mentioned, *Ctsq* is the main molecular marker to identify this cell type by WB or RT-qPCR. They belong to a family of proteolytic enzymes with either serine, aspartic or cysteine protease activities. Cathepsins are involved in the degradation of extracellular matrix proteins to facilitate the remodeling of the spiral arteries mediated by the invasive sinusoidal TGCs, leading to a correct placental perfusion through the labyrinth (Screen *et al*., 2008; Gutiérrez *et al*., 2020). Our data revealed a substantial reduction in the expression of the sinusoidal TGC marker, *Ctsq,* within the *Irs2* KO clones.

Prolactin family 2, subfamily c, member 5 (*Prl2c5*) belongs to the same subfamily of prolactins as *Prl2c2*, which is one of the molecular markers for TGCs. They encode for hormones synthetized by TGCs to induce maternal metabolic adaptations to pregnancy (Napso *et al*., 2018) and ensure vasculature remodeling at the fetal-maternal interface (Hu and Cross, 2010).

Finally, *Nos2* encodes for the nitric oxide synthase 2, a protein which synthetizes the potent vasodilator nitric oxide (NO). It is released by trophoblast cells, contributing to the success of the implantation and invasion process, by helping to maintain vasodilatation and preventing the coagulation of platelets on the trophoblast surface (Gagioti and Bevilacqua, 2000). Lack of NO during gestation is related to the development of pregnancy-induced hypertension and pre-eclampsia (Maul *et al*., 2003).

Overall, our results indicate that the lack of IRS2 during trophoblast differentiation leads to a decrease in sinusoidal TGC markers and factors for tissue remodeling. This suggests that defects in *Irs2* expression might lead to an inadequate vascularization process and placental perfusion, distinctive characteristics of pregnancy complications such as pre-eclampsia and fetal growth restriction.

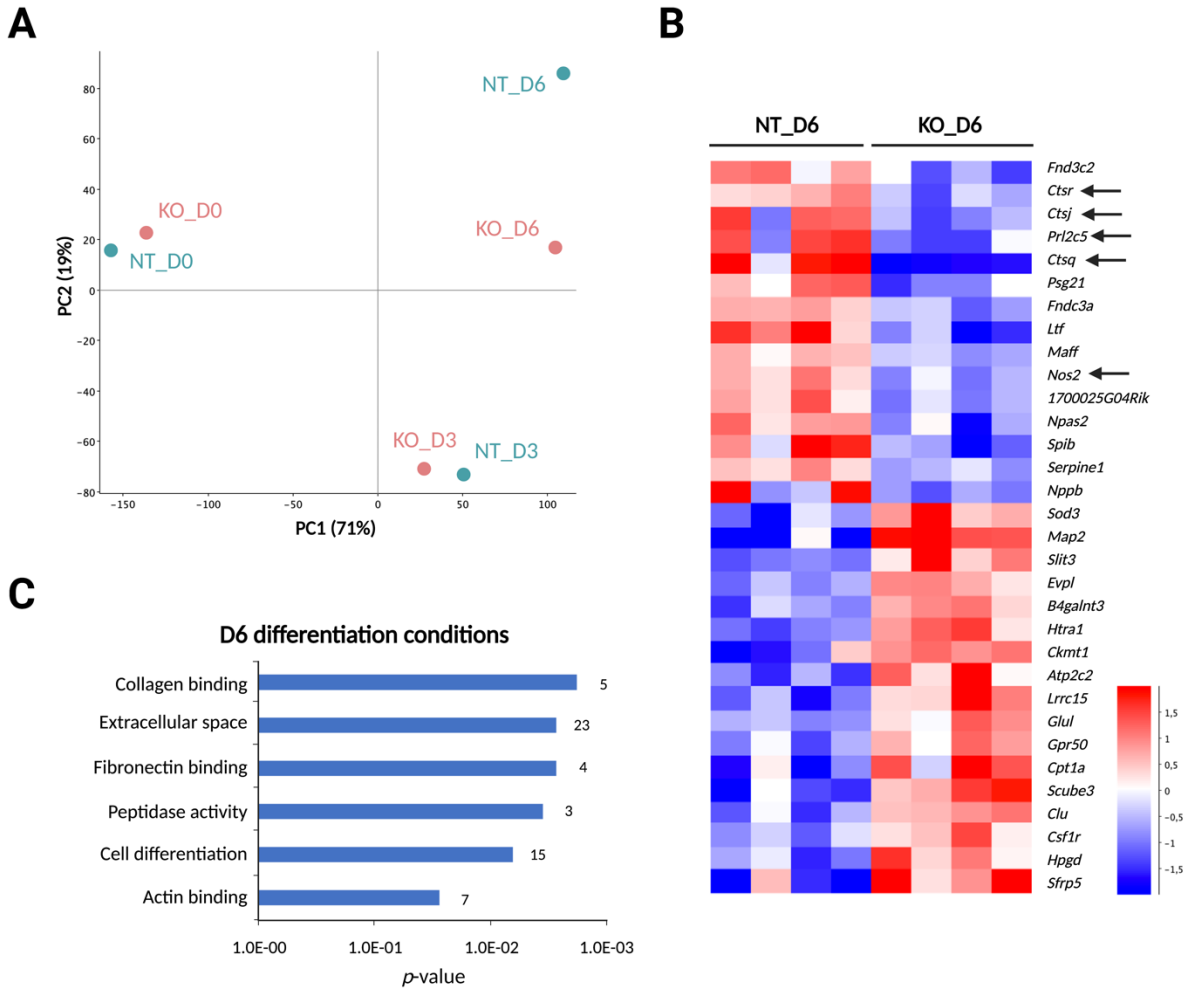

FIGURE 13. Irs2 deficiency affects late trophoblast differentiation (D6). **(A)** Principal component analysis of global transcriptomes of control (NT) and *Irs2* knockout (KO) clones grown in stem cell conditions (D0) and after 3 and 6 days of differentiation (D3 and D6). Each dot represents four independent clones (n = 4) in each differentiation time condition. **(B)** Heatmap of mean row-centered $\log_2$ FPKM values of differentially expressed genes (DESeq2 and intensity difference) in control (NT) and *Irs2* knockout (KO) mTSC clones at day 6 of trophoblast differentiation (D6). Arrows point to genes associated with sinusoidal TGC development, extracellular matrix remodeling and vascularization. Four independent biological replicates per genotype were sequenced. **(C)** Representation of the DAVID output data. Gene ontology analysis of differentially expressed genes (DEGs) between control and *Irs2*-null mTSCs after 6 days of differentiation (D6).

4.3. IRS2 is implicated in PI3K/Akt signaling pathway activated through the IGF axis

In order to explore the impact of depleting *Irs2* on downstream signaling, we decided to perform stimulation experiments in *Irs2* knockout (KO) and control (NT) mTSC clones. As previously explained, IRS2 is involved in the IGF axis, and IGF2 is the most abundantly expressed IGF in the placenta (Sferruzzi-Perri, 2018). Thus, it seemed rational to stimulate with IGF2 and study the signaling pathways activated through IRS2. Upon stimulation with IGF2, this ligand interacts with the IGF1R dimer, promoting its crossed-phosphorylation and subsequent activation, followed by a recruitment of IRS2. We hypothesized that for NT clones, IRS2 downstream effector proteins would be triggered, while in the case of KO clones some form of defect should be seen in the signaling pathway.

Firstly, we confirmed the presence of the IGF system components in trophoblast cells with the RNAseq data that we had (**Figure 14**). The mRNA levels of *Igf1*, *Igf1r* and *Igf2r* are higher in stem cell conditions than upon differentiation and they show similar expression patterns. Meanwhile, *Igf2* shows an upregulation at day 3. This might be due to the fact that *Igf2* is mostly produced by trophoblast cells upon differentiation, by the SynT layer in direct contact with maternal blood (Sferruzzi-Perri *et al*., 2011b). However, studies indicate that it is also expressed in early stages of development, in the blastocyst, and that it is co-localized with IGF1R and IGF2R in the cell lineages that will go on to form the placenta (Sferruzzi-Perri, 2018).

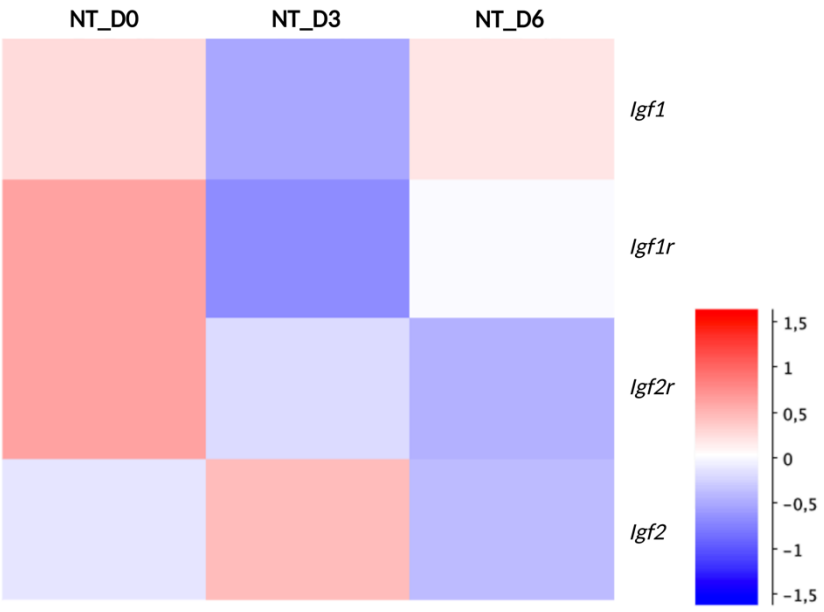

FIGURE 14. Components of the IGF system are highly expressed in mTSCs. Heatmap of *Igf1*, *Igf1r*, *Igf2* and *Igf2r* expression in mTSCs in stem cell conditions (D0) and day 3 (D3) and 6 (D6) of differentiation. Four independent biological replicates per genotype were sequenced.

Although this heatmap compares the expression levels across different days of trophoblast differentiation, it does not provide a comprehensive representation of the total mRNA levels of *Igf2* in mTSCs. To accurately determine *Igf2* mRNA levels, an RT-qPCR analysis would have been more appropriate. However, the current heatmap serves the purpose of confirming the presence of IGF system components in mTSCs before initiating the signaling experiments and stimulating with IGF2.

4.3.1. PI3K/AKT signaling pathway is mediated through IRS2 upon IGF2 stimulation

We synchronized the cellular metabolism by substituting the complete medium with a starving medium lacking FBS, FGF/heparin and conditioned medium. After 8 hours of starvation, stimulation was performed by adding IGF2 (50 ng/mL) to the medium. In order to study early signaling events, IGF2 stimulation was carried out in control compared to *Irs2* KO mTSC clones during 0, 5, 10 and 30 minutes (**Figure 15A**). As expected, IRS2 protein levels are absent for knockout (KO) clones. This outcome provides yet another confirmation of the accurate execution of the genome editing process previously done in the laboratory.

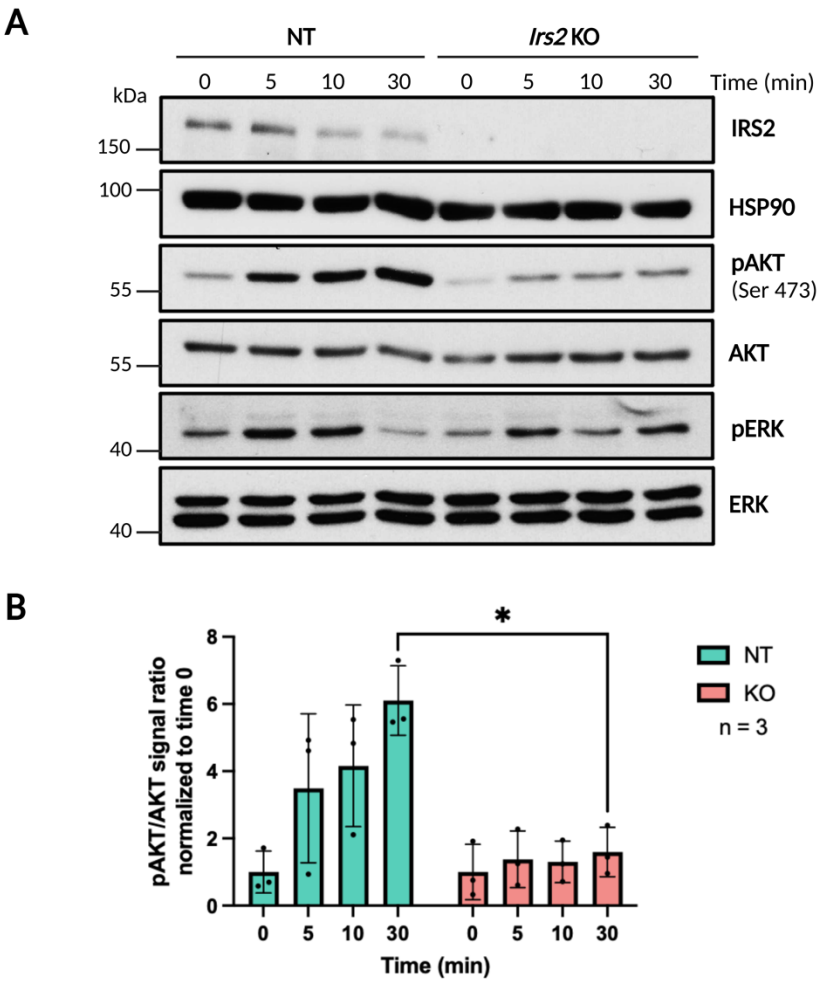

FIGURE 15. PI3K/AKT signaling pathway mediated through IRS2 is activated upon IGF2 stimulation. (A) Western Blot analysis assessing the signaling activated by IGF2 in control (NT) and *Irs2* knockout (KO) mTSC clones. IRS2, pAKT (AKT phosphorylated at serine 473) and pERK protein levels are studied, with respect to HSP90, total AKT and ERK, respectively. Blots are representative of three independent replicates. (B) Quantification of band intensities for pAKT (Ser473) levels. Data are normalized against total AKT and represented relative to starving condition in NT, at time 0; mean ± SEM; * $p < 0,05$ (two-way ANOVA with Šídák's multiple comparisons test).

Regarding signaling, we decided to study the levels of AKT and ERK activated, represented by their phosphorylation and thereby denotated as pAKT (phosphorylated AKT) and pERK (phosphorylated ERK, p42/44). As previously mentioned, the two main signaling pathways activated downstream of

IRS2 are the PI3K/AKT pathway and the MAPK cascade, leading to cell proliferation, survival, differentiation and metabolism regulation (Taniguchi *et al*., 2006; Hiden *et al*., 2009). Therefore, it appeared rational to investigate the expression of pAKT and pERK, which are downstream of these pathways, respectively.

pAKT can be phosphorylated at multiple sites within its protein structure, being threonine 308 (Thr308) and serine 473 (Ser473) the two main ones associated with AKT activation. Thr308 is firstly phosphorylated by phosphoinositide-dependent kinase 1 (PDK1). PDK1 is a serine/threonine kinase that binds to PIP_3, lipid molecules phosphorylated by PI3K, triggering a conformational change and enabling it to phosphorylate AKT (Thr308) (Huang *et al*., 2018). Further phosphorylation is required in Ser473, a phosphorylation often reported to increase AKT *in vitro* activity ten- to hundred-fold (Yudushkin, 2020) with respect to only a Thr308 phosphorylation. This is carried out by the mammalian target of rapamycin complex 2 (mTORC2), which is also activated in a PI3K-dependent manner. pAKT (Ser473) has been particularly associated with cell survival, through the PI3K/AKT signaling pathway induced by growth factors such as the IGFs (Huang *et al*., 2018). Thus, we decided to use antibodies specific to this post-translational modification, since it represents the full AKT activity.

Our results confirm that IGF2 stimulation in mTSCs activates the PI3K/AKT signaling pathway, as evidenced by the significant increase in pAKT protein levels in control (NT) clones following stimulation (**Figure 15A**). However, clones with *Irs2* deficiency (KO) showed a delayed phosphorylation of AKT, with pAKT levels in KO clones not reaching the same extent as in NT clones. Notably, a significant disparity in the amount of AKT activated (pAKT/AKT) between NT and KO clones was observed after 30 minutes of stimulation (**Figure 15B**). This pathway is not completely repressed in *Irs2* KO clones, as some pAKT band intensity is still observed. We hypothesize that it might be due to the presence of other compensatory proteins that supplant the loss of IRS2, like for example its homologous IRS1. Further research is needed to precise potential compensatory mechanisms involving IRS1 in this context.

In contrast, we did not observe any discernible differences in the MAPK pathway, as the levels of phosphorylated ERK (pERK) remained comparable between NT and KO clones (**Figure 15A**). This implies that IGF2 may not be the primary inducer of the MAPK cascade through IRS2 in mTSCs, and alternative growth factors such as fibroblast growth factor (FGF) might play a more substantial role, as indicated by preliminary findings from our laboratory.

To further corroborate these results, we performed an immunofluorescence (IF) staining, in which we marked pAKT with Alexa488, a green fluorochrome. Our data indicate that AKT is phosphorylated upon IGF2 stimulation and that pAKT is localized mainly in the cytosol (**Figure 16A**). Quantification of the fluorescence intensity confirms that the difference between the amount of AKT activated in control (NT) and *Irs2* knockout (KO) clones is statistically significant, being extensively lower for KO clones upon 10 and 30 minutes of IGF2 stimulation (**Figure 16B**).

Overall, our findings indicate that the activation of the PI3K/AKT pathway by IGF2 is mediated through IRS2. This signaling leads to IGF-mediated cell survival and differentiation of trophoblast stem cells (Forbes *et al*., 2008; Lee *et al*., 2019). PI3K/AKT signaling has been formerly reported to regulate the differentiation and invasive properties of trophoblast (Kent *et al*., 2010) and thereby it is involved in placental development. Previous studies in mice, in which the p110α-catalytic subunit of PI3K was knocked out, demonstrate that disrupting p110α activity impairs placental growth and impacts on nutrient transport to the fetus (Sferruzzi-Perri *et al*., 2016; López-Tello *et al*., 2019). In these studies, p110α mutants showed reduced developmental angiogenesis and defective labyrinth morphogenesis, similarly to when knocking out *Igf2* or *Akt* (Kent *et al*., 2012). Alterations in labyrinth morphology result in a compromised ability to effectively transport nutrients from the mother to the fetus, leading to intrauterine growth restriction (IUGR).

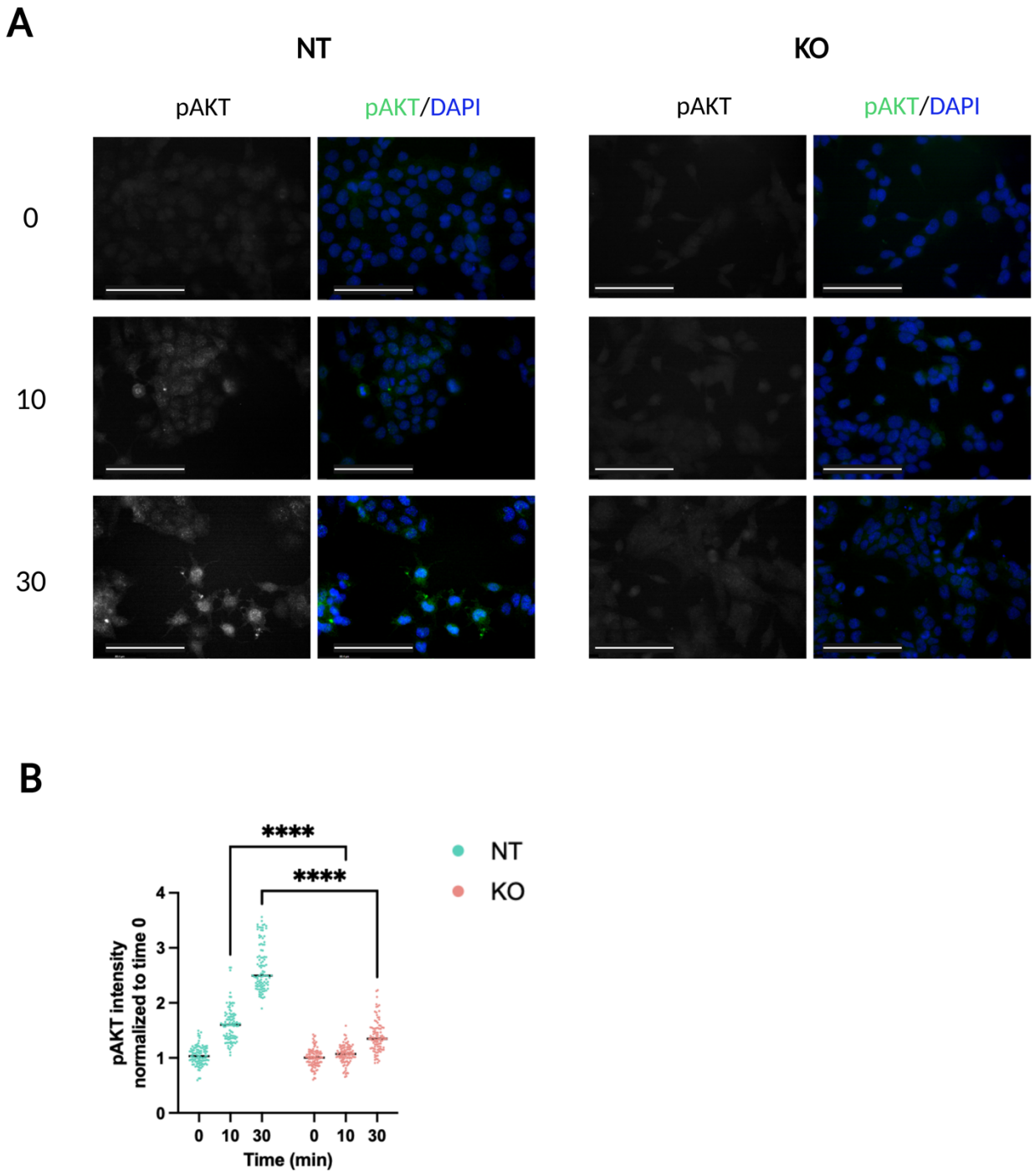

FIGURE 16. IRS2-mediated phosphorylation of AKT in the cytosol upon IGF2 stimulation. **(A)** Immunofluorescence staining of control (NT) and *Irs2* knockout (KO) mouse trophoblast stem cells (mTSCs) for pAKT upon 0, 10 and 30 minutes of IGF2 stimulation. Representative images of three replicates. Scale bar: 100 µm. **(B)** Scatter plot showing pAKT fluorescence intensity per cell in each stimulation condition for NT and KO mTSCs. Quantification of 100 cells in 5 different fields. Data are normalized relative to starving condition in NT, at time 0; **** $p < 0{,}0001$ (two-way ANOVA with Šídák's multiple comparisons test).

We postulate that this could be the underlying cause for the observed 10% size reduction in the offspring of *Irs2* KO litters (Withers *et al*., 1998). We hypothesize that they might also exhibit impairments in IGF2/IRS2/PI3K/AKT signaling, which could subsequently affect cell survival and disrupt placental development, thereby resulting in comparable placental phenotypes to those observed in IGF2, p110α, or AKT mutants. Conducting further research to gain deeper insights into the placental morphology in *Irs2* KO mice would prove invaluable in elucidating whether they also exhibit aberrations within their labyrinth region.

4.3.2. IGF2 performs a redundant role similar to that of IGF1

The observation of downstream signaling effects of IGF2 stimulation through IRS2 raises the question as to which receptor is IGF2 binding to. Our initial hypothesis postulated that IGF2 binds to IGF1R; however, we also considered the possibility of the insulin receptor isoform A (IR_A) playing a role in this context. Therefore, to gain a more detailed understanding of the signaling pathway, we performed a stimulation experiment with IGF1, the growth factor that binds to IGF1R with higher affinity. The rationale behind this approach was to assess whether we would obtain similar results as when stimulating with IGF2, thereby indicating a redundant action of IGF1 and IGF2 through the IGF1R.

We synchronized cell metabolism and performed IGF1 stimulation (100 ng/mL) during 0, 5, 10 and 30 minutes to study early signaling events (**Figure 17A**). Once again, IRS2 protein levels are absent for knockout (KO) clones, confirming the success of the CRISPR genome editing.

In terms of the divergent signaling pathways influenced by the presence or absence of IRS2, our results reveal that IGF1 signals through IRS2 to activate the PI3K/AKT pathway, similarly to the outcomes observed with IGF2 stimulation (**Figure 17A**). In this case, a highly statistically significant disparity is evident in activated AKT protein levels at both 10-minute and 30-minute stimulation time points, exhibiting markedly reduced activation in IRS2-deficient clones. Conversely, regarding the MAPK signaling cascade, it seems that there is a slight decline in the levels of pERK; however, this delay is not statistically significant (**Figure 17B**).

Given the shared signaling characteristics between insulin-like growth factors IGF1 and IGF2, we consider that they show overlapping roles, mediated through IGF1R. Notably, IGF1R is highly expressed in placentas and it co-localized with IGF2 and IGF1 in the syncytiotrophoblast layer of the labyrinth (Sferruzzi-Perri, 2018). Our results further evidence that IGF2 binds to IGF1R, since it promotes the PI3K/AKT pathway, in the same way as IGF1. However, further insight could be gained by employing siRNA targeting IGF1R to silence its expression, followed by IGF2 stimulation. According to our results, the absence of IGF1R would impede signal transduction mediated by IGF2.

Insulin-like growth factors are essential for fetal growth and proper placental morphogenesis. In fact, IGF1 and IGF2 production highly rises during pregnancy (Sferruzzi-Perri *et al.*, 2011b), coming from different sources. As previously stated, the placenta is the highest source of IGF2 (Sferruzzi-Perri, 2018), although it can also be produced by the mother and the fetus. In contrast, IGF1 is expressed very little by the placenta (Han and Carter, 2000). However, the placenta may influence maternal IGF1 production, by secreting hormones, such as the placental growth hormone (PGH), which indirectly modulate IGF1 synthesis in maternal tissues (Alsat *et al*., 1998).

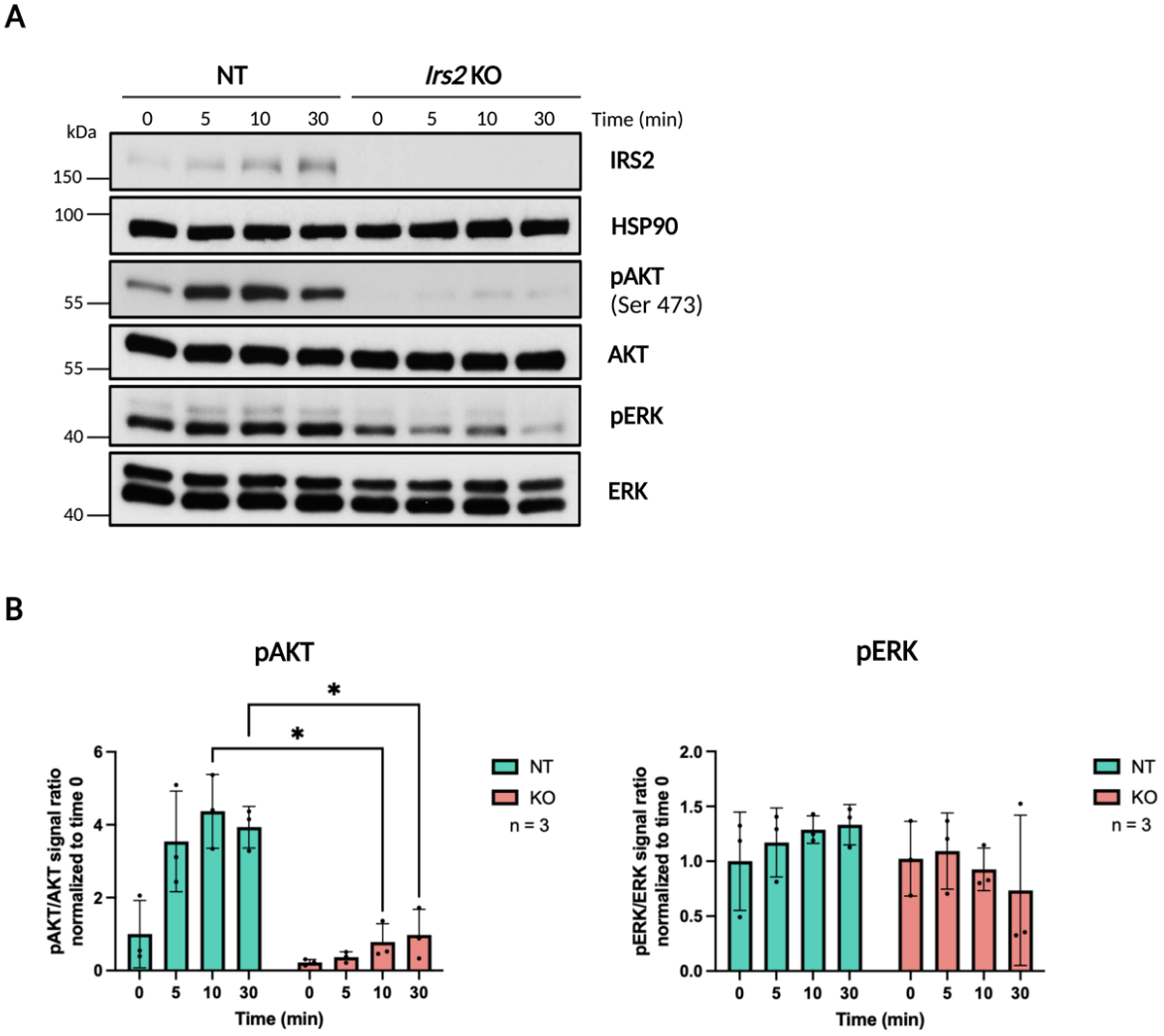

FIGURE 17. IGF2 is redundant to IGF1, which also activates the PI3K/AKT signaling pathway mediated through IRS2. (A) Western Blot analysis assessing the signaling activated by IGF1 in control (NT) and *Irs2* knockout (KO) mTSC clones. IRS2, pAKT (AKT phosphorylated at serine 473) and pERK protein levels are studied, with respect to HSP90, total AKT and ERK, respectively. Blots are representative of three independent replicates. (B) Quantification of band intensities for pAKT (Ser473) levels (left-hand side) and for pERK levels (right-hand side). Data are normalized against total AKT and total ERK, respectively and represented relative to starving condition in NT, at time 0; mean ± SEM; * $p < 0,05$ (two-way ANOVA with Šídák's multiple comparisons test).

Our results indicate that in trophoblast stem cells, IGF1 and IGF2 activate the PI3K/AKT pathway in an IRS2-dependent manner, suggesting an overlapping role of these factors in promoting cell survival, growth and differentiation towards a healthy placenta, thereby permitting a correct fetal development. However, not only can they influence the growth of the placenta, but they can also modulate its function. IGFs can induce the placenta to secrete hormones into the maternal circulation, altering maternal metabolism and substrate availability for placental transfer (Sferruzzi-Perri *et al.*, 2011b). Moreover, studies *in vitro* have proven that IGF1 and IGF2 can stimulate glucose and amino acid uptake in trophoblast (*Karl*, 1995).

Thus, IGFs play a crucial role in promoting placental growth and function. However, in the absence of IRS2, which we have proven to be a key mediator of IGF1 and IGF2 signaling, the role of these growth factors would be impaired, resulting in a notable detriment to placental development and fetal nutrient acquisition and subsequently hampering the overall growth and development of the fetus.

5. CONCLUSION

The placenta is an extraembryonic organ that often goes unnoticed but plays a pivotal role during gestation in nurturing and sustaining the developing life within the womb. Placental insufficiency can result in fetal intrauterine growth restriction (IUGR), with consequences that extend well beyond the prenatal period, exerting long-term effects on the individual's health and well-being into adulthood (Burton and Jauniaux, 2018). Therefore, understanding the molecular mechanisms underlying defective placental development and altered fetal growth is of utmost importance.

One of the main placental and fetal development mediators are the growth factors of the insulin/insulin-like growth factor (IGF) axis. They act on the building cell blocks of the placenta, trophoblast stem cells. Ligands IGF1 and IGF2 have been described to interact with IGF1R, which then transduces the signal intracellularly. IGFs are known to regulate placental morphogenesis, nutrient transport and hormone secretion, hijacking maternal metabolism to meet the demands of the growing fetus (Sferruzzi-Perri *et al.*, 2011b). However, little is known about the precise signaling pathways regulating their effects.

The main objective of this project was to decipher the molecular function of IRS2, a cytosolic docking protein that integrates signals downstream of tyrosine kinase receptors, such as IGF1R, in placental development through a study of mouse trophoblast stem cells (mTSCs). The conclusions drawn from the present work are the following:

1. *Irs2* expression is observed in mTSCs and it is modulated transcriptionally during trophoblast differentiation, suggesting that it plays a role in placental development.
2. *Irs2* knockout (KO) mTSC clones show defects in late trophoblast differentiation. At day 6, they present significantly downregulated genes related to sinusoidal trophoblast giant cell (TGC) development (*Ctsq*, *Ctsr*, *Ctsj),* and vascularization (*Prl2c5*, *Nos2*). This is a clear indicator that IRS2 is essential for proper sinusoidal giant cell differentiation, a specific subpopulation of cells located in the labyrinth, the exchange region between the mother and the fetus.
3. IGF1 and IGF2 play overlapping roles by binding to IGF1R and triggering the PI3K/AKT pathway through the IRS2 cytosolic docking protein in mTSCs. In the absence of *Irs2*, mTSCs show a reduced activation of this signaling pathway, thereby, we confirm that IRS2 is the main mediator of IGFs action in trophoblast development by triggering the PI3K/AKT pathway.

Further research is needed to corroborate the *in silico* findings about IRS2 depletion impairing proper trophoblast differentiation, by assessing *in vivo* morphological defects of *Irs2* KO placentas. It is tempting to speculate that *Irs2* mutants would show defects in the labyrinth morphogenesis, similarly to deficiencies in other components of the signaling axis described, such as *Igf2*, *p110α* and *Akt* mutants (Kent *et al*., 2012; Sferruzzi-Perri *et al*., 2016; López-Tello *et al*., 2019). This would explain the observed 10% size reduction in the offspring of *Irs2* KO litters (Withers *et al*., 1998), as a defective labyrinth region would result in a compromised ability to effectively transport nutrients from the mother to the fetus, leading to fetal growth restriction.

6. REFERENCES

Alsat, E., Guibourdenche, J., Couturier, A., & Evain-Brion, D. (1998). Physiological role of human placental growth hormone. *Molecular and cellular endocrinology*, *140*(1-2), 121–127. https://doi.org/10.1016/s0303-7207(98)00040-9

Brummer, T., Schmitz-Peiffer, C., & Daly, R. J. (2010). Docking proteins. *The FEBS journal*, *277*(21), 4356–4369. https://doi.org/10.1111/j.1742-4658.2010.07865.x

Burks, D. J., Font de Mora, J., Schubert, M., Withers, D. J., Myers, M. G., Towery, H. H., Altamuro, S. L., Flint, C. L., & White, M. F. (2000). IRS-2 pathways integrate female reproduction and energy homeostasis. *Nature*, *407*(6802), 377–382. https://doi.org/10.1038/35030105

Burton, G. J., & Jauniaux, E. (2018). Pathophysiology of placental-derived fetal growth restriction. *American journal of obstetrics and gynecology*, *218*(2S), S745–S761. https://doi.org/10.1016/j.ajog.2017.11.577

Constância, M., Hemberger, M., Hughes, J., Dean, W., Ferguson-Smith, A., Fundele, R., Stewart, F., Kelsey, G., Fowden, A., Sibley, C., & Reik, W. (2002). Placental-specific IGF-II is a major modulator of placental and fetal growth. *Nature*, *417*(6892), 945–948. https://doi.org/10.1038/nature00819

Forbes, B. E., Blyth, A. J., & Wit, J. M. (2020). Disorders of IGFs and IGF-1R signaling pathways. *Molecular and cellular endocrinology*, *518*, 111035. https://doi.org/10.1016/j.mce.2020.111035

Forbes, K., Westwood, M., Baker, P. N., & Aplin, J. D. (2008). Insulin-like growth factor I and II regulate the life cycle of trophoblast in the developing human placenta. *American journal of physiology. Cell physiology, 294*(6), C1313–C1322. https://doi.org/10.1152/ajpcell.00035.2008

Gagioti, S., Scavone, C., & Bevilacqua, E. (2000). Participation of the mouse implanting trophoblast in nitric oxide production during pregnancy. *Biology of reproduction*, *62*(2), 260–268. https://doi.org/10.1095/biolreprod62.2.260

Gutiérrez, J. A., Gómez, I., Chiarello, D. I., Salsoso, R., Klein, A. D., Guzmán-Gutiérrez, E., Toledo, F., & Sobrevia, L. (2020). Role of proteases in dysfunctional placental vascular remodelling in preeclampsia. *Biochimica et biophysica acta. Molecular basis of disease, 1866*(2), 165448. https://doi.org/10.1016/j.bbadis.2019.04.004

Han, V. K., & Carter, A. M. (2000). Spatial and temporal patterns of expression of messenger RNA for insulin-like growth factors and their binding proteins in the placenta of man and laboratory animals. *Placenta*, *21*(4), 289–305. https://doi.org/10.1053/plac.1999.0498

Harris, L. K., Crocker, I. P., Baker, P. N., Aplin, J. D., & Westwood, M. (2011). IGF2 actions on trophoblast in human placenta are regulated by the insulin-like growth factor 2 receptor, which can function as both a signaling and clearance receptor. *Biology of reproduction*, *84*(3), 440–446. https://doi.org/10.1095/biolreprod.110.088195

Harris, L. K., & Westwood, M. (2012). Biology and significance of signalling pathways activated by IGF-II. *Growth factors (Chur, Switzerland)*, *30*(1), 1–12. https://doi.org/10.3109/08977194.2011.640325

Hemberger, M., Hanna, C. W., & Dean, W. (2020). Mechanisms of early placental development in mouse and humans. *Nature reviews. Genetics*, *21*(1), 27–43. https://doi.org/10.1038/s41576-019-0169-4

Hiden, U., Glitzner, E., Hartmann, M., & Desoye, G. (2009). Insulin and the IGF system in the human placenta of normal and diabetic pregnancies. *Journal of anatomy*, *215*(1), 60–68. https://doi.org/10.1111/j.1469-7580.2008.01035.x

Hu, D., & Cross, J. C. (2010). Development and function of trophoblast giant cells in the rodent placenta. *The International journal of developmental biology*, *54*(2-3), 341–354. https://doi.org/10.1387/ijdb.082768dh

Huang, X., Liu, G., Guo, J., & Su, Z. (2018). The PI3K/AKT pathway in obesity and type 2 diabetes. *International journal of biological sciences, 14*(11), 1483–1496. https://doi.org/10.7150/ijbs.27173

Karl P. I. (1995). Insulin-like growth factor-1 stimulates amino acid uptake by the cultured human placental trophoblast. *Journal of cellular physiology*, *165*(1), 83–88. https://doi.org/10.1002/jcp.1041650111

Kent, L. N., Konno, T., & Soares, M. J. (2010). Phosphatidylinositol 3 kinase modulation of trophoblast cell differentiation. *BMC developmental biology, 10*, 97. https://doi.org/10.1186/1471-213X-10-97

Kent, L. N., Ohboshi, S., & Soares, M. J. (2012). Akt1 and insulin-like growth factor 2 (Igf2) regulate placentation and fetal/postnatal development. *The International journal of developmental biology*, *56*(4), 255–261. https://doi.org/10.1387/ijdb.113407lk

Knöfler, M., Haider, S., Saleh, L., Pollheimer, J., Gamage, T. K. J. B., & James, J. (2019). Human placenta and trophoblast development: key molecular mechanisms and model systems. *Cellular and molecular life sciences : CMLS*, *76*(18), 3479–3496. https://doi.org/10.1007/s00018-019-03104-6

Latos, P. A., & Hemberger, M. (2014). Review: the transcriptional and signalling networks of mouse trophoblast stem cells. *Placenta*, *35 Suppl*, S81–S85. https://doi.org/10.1016/j.placenta.2013.10.013

Latos, P. A., & Hemberger, M. (2016). From the stem of the placental tree: trophoblast stem cells and their progeny. *Development (Cambridge, England), 143*(20), 3650–3660. https://doi.org/10.1242/dev.133462

Lee, C. Q. E., Bailey, A., Lopez-Tello, J., Sferruzzi-Perri, A. N., Okkenhaug, K., Moffett, A., Rossant, J., & Hemberger, M. (2019). Inhibition of Phosphoinositide-3-Kinase Signaling Promotes the Stem Cell State of Trophoblast. *Stem cells (Dayton, Ohio), 37*(10), 1307–1318. https://doi.org/10.1002/stem.3052

López-Tello, J., Pérez-García, V., Khaira, J., Kusinski, L. C., Cooper, W. N., Andreani, A., Grant, I., Fernández de Liger, E., Lam, B. Y., Hemberger, M., Sandovici, I., Constancia, M., & Sferruzzi-Perri, A. N. (2019). Fetal and trophoblast PI3K p110α have distinct roles in regulating resource supply to the growing fetus in mice. *eLife*, *8*, e45282. https://doi.org/10.7554/eLife.45282

Maltepe, E., & Fisher, S. J. (2015). Placenta: the forgotten organ. *Annual review of cell and developmental biology*, *31*, 523–552. https://doi.org/10.1146/annurev-cellbio-100814-125620

Mardilovich, K., Pankratz, S. L., & Shaw, L. M. (2009). Expression and function of the insulin receptor substrate proteins in cancer. *Cell communication and signaling : CCS*, *7*, 14. https://doi.org/10.1186/1478-811X-7-14

Mason R. W. (2008). Emerging functions of placental cathepsins. *Placenta, 29*(5), 385–390. https://doi.org/10.1016/j.placenta.2008.02.006

Maul, H., Longo, M., Saade, G. R., & Garfield, R. E. (2003). Nitric oxide and its role during pregnancy: from ovulation to delivery. *Current pharmaceutical design, 9*(5), 359–380. https://doi.org/10.2174/1381612033391784

Napso, T., Yong, H. E. J., Lopez-Tello, J., & Sferruzzi-Perri, A. N. (2018). The Role of Placental Hormones in Mediating Maternal Adaptations to Support Pregnancy and Lactation. *Frontiers in physiology*, *9*, 1091. https://doi.org/10.3389/fphys.2018.01091

NCBI [Internet]. National Center for Biotechnology Information. 2023. [Access 15th of May 2023]. Available from: https://www.ncbi.nlm.nih.gov/

Oliveira, J. M., Rebuffat, S. A., Gasa, R., & Gomis, R. (2014). Targeting type 2 diabetes: lessons from a knockout model of insulin receptor substrate 2. *Canadian journal of physiology and pharmacology*, *92*(8), 613–620. https://doi.org/10.1139/cjpp-2014-0114

Pérez-García, V., Fineberg, E., Wilson, R., Murray, A., Mazzeo, C. I., Tudor, C., Sienerth, A., White, J. K., Tuck, E., Ryder, E. J., Gleeson, D., Siragher, E., Wardle-Jones, H., Staudt, N., Wali, N., Collins, J., Geyer, S., Busch-Nentwich, E. M., Galli, A., Smith, J. C., … Hemberger, M. (2018). Placentation defects are highly prevalent in embryonic lethal mouse mutants. *Nature, 555*(7697), 463–468. https://doi.org/10.1038/nature26002

Randhawa, R., & Cohen, P. (2005). The role of the insulin-like growth factor system in prenatal growth. *Molecular genetics and metabolism*, *86*(1-2), 84–90. https://doi.org/10.1016/j.ymgme.2005.07.028

Renaud, S. J., Karim Rumi, M. A., & Soares, M. J. (2011). Review: Genetic manipulation of the rodent placenta. *Placenta*, *32 Suppl 2*(Suppl 2), S130–S135. https://doi.org/10.1016/j.placenta.2010.12.017

Roberts, R. M., & Fisher, S. J. (2011). Trophoblast stem cells. *Biology of reproduction*, *84*(3), 412–421. https://doi.org/10.1095/biolreprod.110.088724

Sandovici, I., Georgopoulou, A., Pérez-García, V., Hufnagel, A., López-Tello, J., Lam, B. Y. H., Schiefer, S. N., Gaudreau, C., Santos, F., Hoelle, K., Yeo, G. S. H., Burling, K., Reiterer, M., Fowden, A. L., Burton, G. J., Branco, C. M., Sferruzzi-Perri, A. N., & Constância, M. (2022). The imprinted Igf2-Igf2r axis is critical for matching placental microvasculature expansion to fetal growth. *Developmental cell*, *57*(1), 63–79.e8. https://doi.org/10.1016/j.devcel.2021.12.005

Screen, M., Dean, W., Cross, J. C., & Hemberger, M. (2008). Cathepsin proteases have distinct roles in trophoblast function and vascular remodelling. *Development (Cambridge, England), 135*(19), 3311–3320. https://doi.org/10.1242/dev.025627

Sferruzzi-Perri A. N. (2018). Regulating needs: Exploring the role of insulin-like growth factor-2 signalling in materno-fetal resource allocation. *Placenta*, *64 Suppl 1*, S16–S22. https://doi.org/10.1016/j.placenta.2018.01.005

Sferruzzi-Perri, A. N., López-Tello, J., Fowden, A. L., & Constancia, M. (2016). Maternal and fetal genomes interplay through phosphoinositol 3-kinase(PI3K)-p110α signaling to modify placental resource allocation. *Proceedings of the National Academy of Sciences of the United States of America*, *113*(40), 11255–11260. https://doi.org/10.1073/pnas.1602012113

Sferruzzi-Perri, A. N., Owens, J. A., Pringle, K. G., & Roberts, C. T. (2011). The neglected role of insulin-like growth factors in the maternal circulation regulating fetal growth. *The Journal of physiology, 589*(Pt 1), 7–20. https://doi.org/10.1113/jphysiol.2010.198622

Sferruzzi-Perri, A. N., Vaughan, O. R., Coan, P. M., Suciu, M. C., Darbyshire, R., Constancia, M., Burton, G. J., & Fowden, A. L. (2011). Placental-specific Igf2 deficiency alters developmental adaptations to undernutrition in mice. *Endocrinology*, *152*(8), 3202–3212. https://doi.org/10.1210/en.2011-0240

Sun, X. J., Wang, L. M., Zhang, Y., Yenush, L., Myers, M. G., Jr, Glasheen, E., Lane, W. S., Pierce, J. H., & White, M. F. (1995). Role of IRS-2 in insulin and cytokine signalling. *Nature*, *377*(6545), 173–177. https://doi.org/10.1038/377173a0

Taniguchi, C. M., Emanuelli, B., & Kahn, C. R. (2006). Critical nodes in signalling pathways: insights into insulin action. *Nature reviews. Molecular cell biology*, *7*(2), 85–96. https://doi.org/10.1038/nrm1837

UNIPROT [Internet]. Universal Protein Knowledgebase. 2023. [Access 15th of May 2023]. Available from: https://www.uniprot.org/

Withers, D. J., Gutierrez, J. S., Towery, H., Burks, D. J., Ren, J. M., Previs, S., Zhang, Y., Bernal, D., Pons, S., Shulman, G. I., Bonner-Weir, S., & White, M. F. (1998). Disruption of IRS-2 causes type 2 diabetes in mice. *Nature*, *391*(6670), 900–904. https://doi.org/10.1038/36116

Woods, L., Pérez-García, V., & Hemberger, M. (2018). Regulation of Placental Development and Its Impact on Fetal Growth-New Insights From Mouse Models. *Frontiers in endocrinology*, *9*, 570. https://doi.org/10.3389/fendo.2018.00570

Yudushkin I. (2020). Control of Akt activity and substrate phosphorylation in cells. *IUBMB life*, *72*(6), 1115–1125. https://doi.org/10.1002/iub.2264

Appendices

Appendix I. Relationship of this work with the Sustainable Development Goals (SDG) of the 2030 Agenda.

Sustainable Development Goals	High	Medium	Low	Not applicable
SDG 1. **No Poverty**				X
SDG 2. **Zero Hunger**				X
SDG 3. **Good Health and Well-being**	X			
SDG 4. **Quality Education**		X		
SDG 5. **Gender Equality**			X	
SDG 6. **Clean Water and Sanitation**				X
SDG 7. **Affordable and Clean Energy**				X
SDG 8. **Decent Work and Economic Growth**				X
SDG 9. **Industry, Innovation and Infrastructure**				X
SDG 10. **Reduced Inequality**			X	
SDG 11. **Sustainable Cities and Communities**				X
SDG 12. **Responsible Consumption and Production**				X
SDG 13. **Climate Action**				X
SDG 14. **Life Below Water**				X
SDG 15. **Life on Land**				X
SDG 16. **Peace and Justice Strong Institutions**				X
SDG 17. **Partnerships to achieve the Goal**				X

Description of the alignment of this work with the SDGs with a high degree of relationship.

SDG 3 aims to ensure healthy lives and promote well-being for all at all ages. It encompasses various objectives, including reducing maternal and child mortality and enhancing the understanding of the underlying mechanisms of health and disease.

This work explores the role of *Irs2*, a protein involved in signaling during placentation. By studying the relationship between *Irs2* and placentation, we have contributed to a better understanding of the molecular mechanisms underlying healthy pregnancies.

Advancing knowledge in this area can have important implications for the prevention and management of complications during pregnancy, such as gestational diabetes and impaired placental function, thereby potentially improving maternal and child health outcomes. Ultimately, it aligns with the broader objective of promoting good health and well-being, as outlined in SDG 3.